SPM

Summary for Policymakers

Drafting Authors:

Lisa V. Alexander (Australia), Simon K. Allen (Switzerland/New Zealand), Nathaniel L. Bindoff (Australia), François-Marie Bréon (France), John A. Church (Australia), Ulrich Cubasch (Germany), Seita Emori (Japan), Piers Forster (UK), Pierre Friedlingstein (UK/Belgium), Nathan Gillett (Canada), Jonathan M. Gregory (UK), Dennis L. Hartmann (USA), Eystein Jansen (Norway), Ben Kirtman (USA), Reto Knutti (Switzerland), Krishna Kumar Kanikicharla (India), Peter Lemke (Germany), Jochem Marotzke (Germany), Valérie Masson-Delmotte (France), Gerald A. Meehl (USA), Igor I. Mokhov (Russian Federation), Shilong Piao (China), Gian-Kasper Plattner (Switzerland), Qin Dahe (China), Venkatachalam Ramaswamy (USA), David Randall (USA), Monika Rhein (Germany), Maisa Rojas (Chile), Christopher Sabine (USA), Drew Shindell (USA), Thomas F. Stocker (Switzerland), Lynne D. Talley (USA), David G. Vaughan (UK), Shang-Ping Xie (USA)

Draft Contributing Authors:

Myles R. Allen (UK), Olivier Boucher (France), Don Chambers (USA), Jens Hesselbjerg Christensen (Denmark), Philippe Ciais (France), Peter U. Clark (USA), Matthew Collins (UK), Josefino C. Comiso (USA), Viviane Vasconcellos de Menezes (Australia/Brazil), Richard A. Feely (USA), Thierry Fichefet (Belgium), Arlene M. Fiore (USA), Gregory Flato (Canada), Jan Fuglestvedt (Norway), Gabriele Hegerl (UK/Germany), Paul J. Hezel (Belgium/USA), Gregory C. Johnson (USA), Georg Kaser (Austria/Italy), Vladimir Kattsov (Russian Federation), John Kennedy (UK), Albert M. G. Klein Tank (Netherlands), Corinne Le Quéré (UK), Gunnar Myhre (Norway), Timothy Osborn (UK), Antony J. Payne (UK), Judith Perlwitz (USA), Scott Power (Australia), Michael Prather (USA), Stephen R. Rintoul (Australia), Joeri Rogelj (Switzerland/Belgium), Matilde Rusticucci (Argentina), Michael Schulz (Germany), Jan Sedláček (Switzerland), Peter A. Stott (UK), Rowan Sutton (UK), Peter W. Thorne (USA/Norway/UK), Donald Wuebbles (USA)

This Summary for Policymakers should be cited as:

IPCC, 2013: Summary for Policymakers. In: *Climate Change 2013: The Physical Science Basis. Contribution of Working Group I to the Fifth Assessment Report of the Intergovernmental Panel on Climate Change* [Stocker, T.F., D. Qin, G.-K. Plattner, M. Tignor, S.K. Allen, J. Boschung, A. Nauels, Y. Xia, V. Bex and P.M. Midgley (eds.)]. Cambridge University Press, Cambridge, United Kingdom and New York, NY, USA.

A. Introduction

The Working Group I contribution to the IPCC's Fifth Assessment Report (AR5) considers new evidence of climate change based on many independent scientific analyses from observations of the climate system, paleoclimate archives, theoretical studies of climate processes and simulations using climate models. It builds upon the Working Group I contribution to the IPCC's Fourth Assessment Report (AR4), and incorporates subsequent new findings of research. As a component of the fifth assessment cycle, the IPCC Special Report on Managing the Risks of Extreme Events and Disasters to Advance Climate Change Adaptation (SREX) is an important basis for information on changing weather and climate extremes.

This Summary for Policymakers (SPM) follows the structure of the Working Group I report. The narrative is supported by a series of overarching highlighted conclusions which, taken together, provide a concise summary. Main sections are introduced with a brief paragraph in italics which outlines the methodological basis of the assessment.

The degree of certainty in key findings in this assessment is based on the author teams' evaluations of underlying scientific understanding and is expressed as a qualitative level of confidence (from *very low* to *very high*) and, when possible, probabilistically with a quantified likelihood (from *exceptionally unlikely* to *virtually certain*). Confidence in the validity of a finding is based on the type, amount, quality, and consistency of evidence (e.g., data, mechanistic understanding, theory, models, expert judgment) and the degree of agreement[1]. Probabilistic estimates of quantified measures of uncertainty in a finding are based on statistical analysis of observations or model results, or both, and expert judgment[2]. Where appropriate, findings are also formulated as statements of fact without using uncertainty qualifiers. (See Chapter 1 and Box TS.1 for more details about the specific language the IPCC uses to communicate uncertainty).

The basis for substantive paragraphs in this Summary for Policymakers can be found in the chapter sections of the underlying report and in the Technical Summary. These references are given in curly brackets.

B. Observed Changes in the Climate System

Observations of the climate system are based on direct measurements and remote sensing from satellites and other platforms. Global-scale observations from the instrumental era began in the mid-19th century for temperature and other variables, with more comprehensive and diverse sets of observations available for the period 1950 onwards. Paleoclimate reconstructions extend some records back hundreds to millions of years. Together, they provide a comprehensive view of the variability and long-term changes in the atmosphere, the ocean, the cryosphere, and the land surface.

Warming of the climate system is unequivocal, and since the 1950s, many of the observed changes are unprecedented over decades to millennia. The atmosphere and ocean have warmed, the amounts of snow and ice have diminished, sea level has risen, and the concentrations of greenhouse gases have increased (see Figures SPM.1, SPM.2, SPM.3 and SPM.4). {2.2, 2.4, 3.2, 3.7, 4.2–4.7, 5.2, 5.3, 5.5–5.6, 6.2, 13.2}

[1] In this Summary for Policymakers, the following summary terms are used to describe the available evidence: limited, medium, or robust; and for the degree of agreement: low, medium, or high. A level of confidence is expressed using five qualifiers: very low, low, medium, high, and very high, and typeset in italics, e.g., *medium confidence*. For a given evidence and agreement statement, different confidence levels can be assigned, but increasing levels of evidence and degrees of agreement are correlated with increasing confidence (see Chapter 1 and Box TS.1 for more details).

[2] In this Summary for Policymakers, the following terms have been used to indicate the assessed likelihood of an outcome or a result: virtually certain 99–100% probability, very likely 90–100%, likely 66–100%, about as likely as not 33–66%, unlikely 0–33%, very unlikely 0–10%, exceptionally unlikely 0–1%. Additional terms (extremely likely: 95–100%, more likely than not >50–100%, and extremely unlikely 0–5%) may also be used when appropriate. Assessed likelihood is typeset in italics, e.g., *very likely* (see Chapter 1 and Box TS.1 for more details).

B.1 Atmosphere

Each of the last three decades has been successively warmer at the Earth's surface than any preceding decade since 1850 (see Figure SPM.1). In the Northern Hemisphere, 1983–2012 was *likely* the warmest 30-year period of the last 1400 years (*medium confidence*). {2.4, 5.3}

- The globally averaged combined land and ocean surface temperature data as calculated by a linear trend, show a warming of 0.85 [0.65 to 1.06] °C[3], over the period 1880 to 2012, when multiple independently produced datasets exist. The total increase between the average of the 1850–1900 period and the 2003–2012 period is 0.78 [0.72 to 0.85] °C, based on the single longest dataset available[4] (see Figure SPM.1). {2.4}

- For the longest period when calculation of regional trends is sufficiently complete (1901 to 2012), almost the entire globe has experienced surface warming (see Figure SPM.1). {2.4}

- In addition to robust multi-decadal warming, global mean surface temperature exhibits substantial decadal and interannual variability (see Figure SPM.1). Due to natural variability, trends based on short records are very sensitive to the beginning and end dates and do not in general reflect long-term climate trends. As one example, the rate of warming over the past 15 years (1998–2012; 0.05 [–0.05 to 0.15] °C per decade), which begins with a strong El Niño, is smaller than the rate calculated since 1951 (1951–2012; 0.12 [0.08 to 0.14] °C per decade)[5]. {2.4}

- Continental-scale surface temperature reconstructions show, with *high confidence*, multi-decadal periods during the Medieval Climate Anomaly (year 950 to 1250) that were in some regions as warm as in the late 20th century. These regional warm periods did not occur as coherently across regions as the warming in the late 20th century (*high confidence*). {5.5}

- It is *virtually certain* that globally the troposphere has warmed since the mid-20th century. More complete observations allow greater confidence in estimates of tropospheric temperature changes in the extratropical Northern Hemisphere than elsewhere. There is *medium confidence* in the rate of warming and its vertical structure in the Northern Hemisphere extra-tropical troposphere and *low confidence* elsewhere. {2.4}

- *Confidence* in precipitation change averaged over global land areas since 1901 is *low* prior to 1951 and *medium* afterwards. Averaged over the mid-latitude land areas of the Northern Hemisphere, precipitation has increased since 1901 (*medium confidence* before and *high confidence* after 1951). For other latitudes area-averaged long-term positive or negative trends have *low confidence* (see Figure SPM.2). {TS TFE.1, Figure 2; 2.5}

- Changes in many extreme weather and climate events have been observed since about 1950 (see Table SPM.1 for details). It is *very likely* that the number of cold days and nights has decreased and the number of warm days and nights has increased on the global scale[6]. It is *likely* that the frequency of heat waves has increased in large parts of Europe, Asia and Australia. There are *likely* more land regions where the number of heavy precipitation events has increased than where it has decreased. The frequency or intensity of heavy precipitation events has *likely* increased in North America and Europe. In other continents, *confidence* in changes in heavy precipitation events is at most *medium*. {2.6}

---

[3] In the WGI contribution to the AR5, uncertainty is quantified using 90% uncertainty intervals unless otherwise stated. The 90% uncertainty interval, reported in square brackets, is expected to have a 90% likelihood of covering the value that is being estimated. Uncertainty intervals are not necessarily symmetric about the corresponding best estimate. A best estimate of that value is also given where available.

[4] Both methods presented in this bullet were also used in AR4. The first calculates the difference using a best fit linear trend of all points between 1880 and 2012. The second calculates the difference between averages for the two periods 1850–1900 and 2003–2012. Therefore, the resulting values and their 90% uncertainty intervals are not directly comparable. {2.4}

[5] Trends for 15-year periods starting in 1995, 1996, and 1997 are 0.13 [0.02 to 0.24] °C per decade, 0.14 [0.03 to 0.24] °C per decade, and, 0.07 [–0.02 to 0.18] °C per decade, respectively.

[6] See the Glossary for the definition of these terms: cold days/cold nights, warm days/warm nights, heat waves.

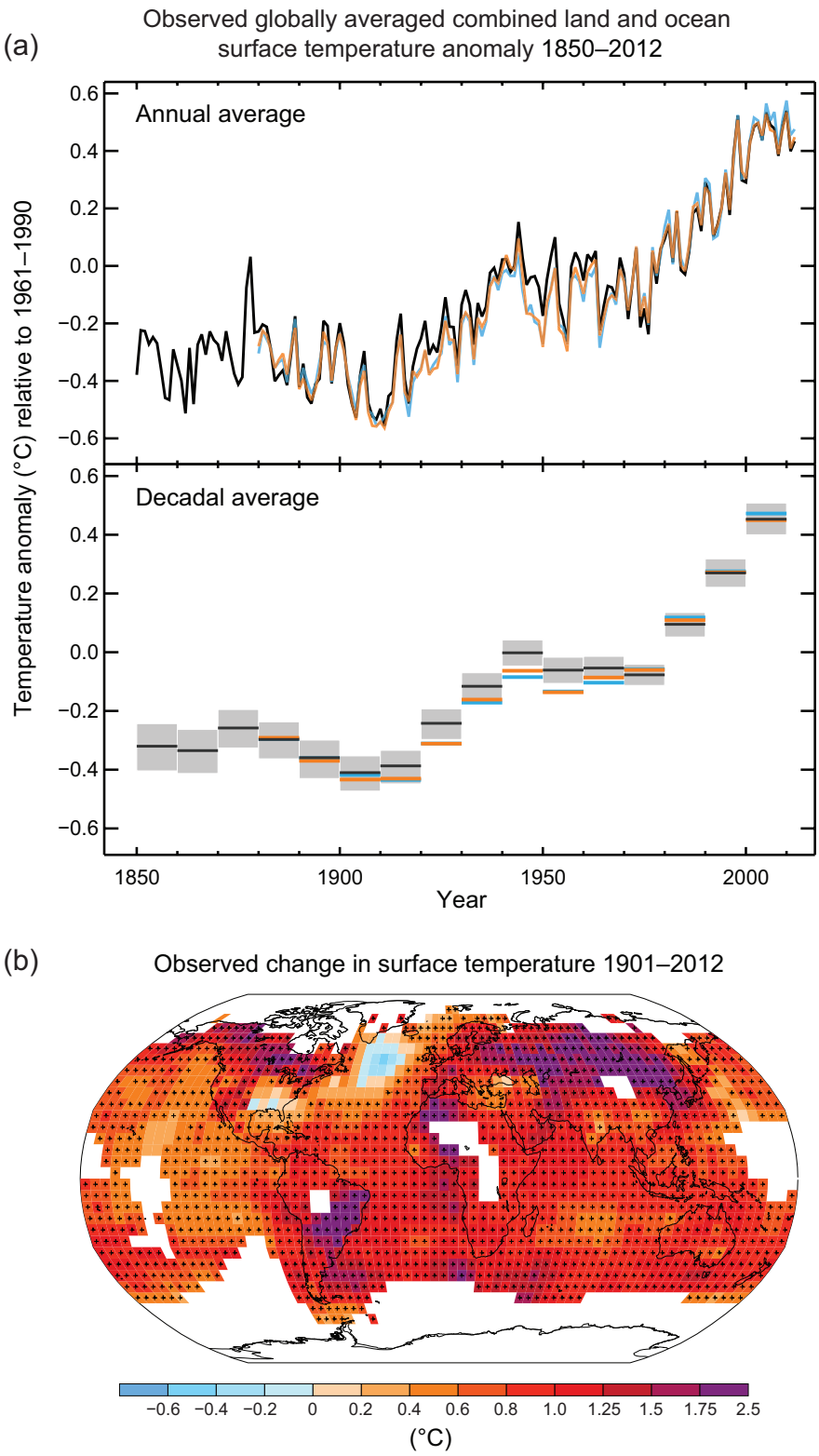

Figure SPM.1 | (a) Observed global mean combined land and ocean surface temperature anomalies, from 1850 to 2012 from three data sets. Top panel: annual mean values. Bottom panel: decadal mean values including the estimate of uncertainty for one dataset (black). Anomalies are relative to the mean of 1961–1990. (b) Map of the observed surface temperature change from 1901 to 2012 derived from temperature trends determined by linear regression from one dataset (orange line in panel a). Trends have been calculated where data availability permits a robust estimate (i.e., only for grid boxes with greater than 70% complete records and more than 20% data availability in the first and last 10% of the time period). Other areas are white. Grid boxes where the trend is significant at the 10% level are indicated by a + sign. For a listing of the datasets and further technical details see the Technical Summary Supplementary Material. {Figures 2.19–2.21; Figure TS.2}

Table SPM.1 | Extreme weather and climate events: Global-scale assessment of recent observed changes, human contribution to the changes, and projected further changes for the early (2016–2035) and late (2081–2100) 21st century. Bold indicates where the AR5 (black) provides a revised* global-scale assessment from the SREX (blue) or AR4 (red). Projections for early 21st century were not provided in previous assessment reports. Projections in the AR5 are relative to the reference period of 1986–2005, and use the new Representative Concentration Pathway (RCP) scenarios (see Box SPM.1) unless otherwise specified. See the Glossary for definitions of extreme weather and climate events.

Phenomenon and direction of trend	Assessment that changes occurred (typically since 1950 unless otherwise indicated)	Assessment of a human contribution to observed changes	Likelihood of further changes	
			Early 21st century	Late 21st century
Warmer and/or fewer cold days and nights over most land areas	*Very likely* {2.6} *Very likely* *Very likely*	***Very likely*** {10.6} *Likely* *Likely*	*Likely* {11.3}	*Virtually certain* {12.4} *Virtually certain* *Virtually certain*
Warmer and/or more frequent hot days and nights over most land areas	*Very likely* {2.6} *Very likely* *Very likely*	***Very likely*** {10.6} *Likely* *Likely* (nights only)	*Likely* {11.3}	*Virtually certain* {12.4} *Virtually certain* *Virtually certain*
Warm spells/heat waves. Frequency and/or duration increases over most land areas	***Medium confidence*** on a global scale *Likely* in large parts of Europe, Asia and Australia {2.6} *Medium confidence* in many (but not all) regions *Likely*	***Likely***[a] {10.6} Not formally assessed *More likely than not*	Not formally assessed[b] {11.3}	*Very likely* {12.4} *Very likely* *Very likely*
Heavy precipitation events. Increase in the frequency, intensity, and/or amount of heavy precipitation	*Likely* more land areas with increases than decreases[c] {2.6} *Likely* more land areas with increases than decreases *Likely* over most land areas	***Medium confidence*** {7.6, 10.6} *Medium confidence* *More likely than not*	*Likely* over many land areas {11.3}	***Very likely*** over most of the mid-latitude land masses and over wet tropical regions {12.4} *Likely* over many areas *Very likely* over most land areas
Increases in intensity and/or duration of drought	***Low confidence*** on a global scale *Likely* changes in some regions[d] {2.6} *Medium confidence* in some regions *Likely* in many regions, since 1970[e]	***Low confidence*** {10.6} *Medium confidence*[f] *More likely than not*	*Low confidence*[g] {11.3}	***Likely*** *(medium confidence)* on a regional to global scale[h] {12.4} *Medium confidence* in some regions *Likely*[e]
Increases in intense tropical cyclone activity	***Low confidence*** in long term (centennial) changes *Virtually certain* in North Atlantic since 1970 {2.6} *Low confidence* *Likely* in some regions, since 1970	***Low confidence***[i] {10.6} *Low confidence* *More likely than not*	*Low confidence* {11.3}	***More likely than not*** in the Western North Pacific and North Atlantic[j] {14.6} *More likely than not* in some basins *Likely*
Increased incidence and/or magnitude of extreme high sea level	*Likely* (since 1970) {3.7} *Likely* (late 20th century) *Likely*	***Likely***[k] {3.7} *Likely*[k] *More likely than not*[k]	*Likely*[l] {13.7}	***Very likely***[l] {13.7} *Very likely*[m] *Likely*

* The direct comparison of assessment findings between reports is difficult. For some climate variables, different aspects have been assessed, and the revised guidance note on uncertainties has been used for the SREX and AR5. The availability of new information, improved scientific understanding, continued analyses of data and models, and specific differences in methodologies applied in the assessed studies, all contribute to revised assessment findings.

Notes:

[a] Attribution is based on available case studies. It is *likely* that human influence has more than doubled the probability of occurrence of some observed heat waves in some locations.

[b] Models project near-term increases in the duration, intensity and spatial extent of heat waves and warm spells.

[c] In most continents, *confidence* in trends is not higher than *medium* except in North America and Europe where there have been *likely* increases in either the frequency or intensity of heavy precipitation with some seasonal and/or regional variation. It is *very likely* that there have been increases in central North America.

[d] The frequency and intensity of drought has *likely* increased in the Mediterranean and West Africa, and *likely* decreased in central North America and north-west Australia.

[e] AR4 assessed the area affected by drought.

[f] SREX assessed *medium confidence* that anthropogenic influence had contributed to some changes in the drought patterns observed in the second half of the 20th century, based on its attributed impact on precipitation and temperature changes. SREX assessed *low confidence* in the attribution of changes in droughts at the level of single regions.

[g] There is *low confidence* in projected changes in soil moisture.

[h] Regional to global-scale projected decreases in soil moisture and increased agricultural drought are *likely (medium confidence)* in presently dry regions by the end of this century under the RCP8.5 scenario. Soil moisture drying in the Mediterranean, Southwest US and southern African regions is consistent with projected changes in Hadley circulation and increased surface temperatures, so there is *high confidence* in *likely* surface drying in these regions by the end of this century under the RCP8.5 scenario.

[i] There is *medium confidence* that a reduction in aerosol forcing over the North Atlantic has contributed at least in part to the observed increase in tropical cyclone activity since the 1970s in this region.

[j] Based on expert judgment and assessment of projections which use an SRES A1B (or similar) scenario.

[k] Attribution is based on the close relationship between observed changes in extreme and mean sea level.

[l] There is *high confidence* that this increase in extreme high sea level will primarily be the result of an increase in mean sea level. There is *low confidence* in region-specific projections of storminess and associated storm surges.

[m] SREX assessed it to be *very likely* that mean sea level rise will contribute to future upward trends in extreme coastal high water levels.

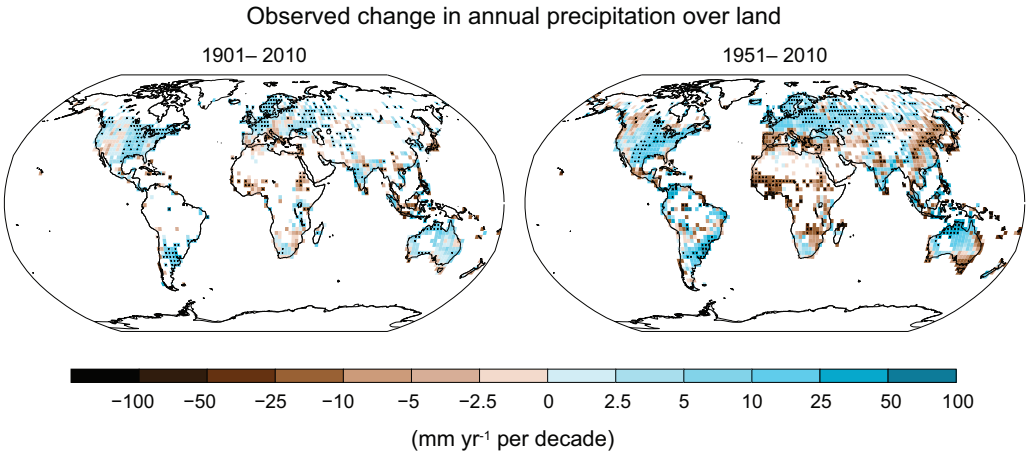

Figure SPM.2 | Maps of observed precipitation change from 1901 to 2010 and from 1951 to 2010 (trends in annual accumulation calculated using the same criteria as in Figure SPM.1) from one data set. For further technical details see the Technical Summary Supplementary Material. {TS TFE.1, Figure 2; Figure 2.29}

B.2 Ocean

Ocean warming dominates the increase in energy stored in the climate system, accounting for more than 90% of the energy accumulated between 1971 and 2010 (*high confidence*). It is *virtually certain* that the upper ocean (0–700 m) warmed from 1971 to 2010 (see Figure SPM.3), and it *likely* warmed between the 1870s and 1971. {3.2, Box 3.1}

- On a global scale, the ocean warming is largest near the surface, and the upper 75 m warmed by 0.11 [0.09 to 0.13] °C per decade over the period 1971 to 2010. Since AR4, instrumental biases in upper-ocean temperature records have been identified and reduced, enhancing confidence in the assessment of change. {3.2}

- It is *likely* that the ocean warmed between 700 and 2000 m from 1957 to 2009. Sufficient observations are available for the period 1992 to 2005 for a global assessment of temperature change below 2000 m. There were *likely* no significant observed temperature trends between 2000 and 3000 m for this period. It is *likely* that the ocean warmed from 3000 m to the bottom for this period, with the largest warming observed in the Southern Ocean. {3.2}

- More than 60% of the net energy increase in the climate system is stored in the upper ocean (0–700 m) during the relatively well-sampled 40-year period from 1971 to 2010, and about 30% is stored in the ocean below 700 m. The increase in upper ocean heat content during this time period estimated from a linear trend is *likely* 17 [15 to 19] × 10^{22} J [7] (see Figure SPM.3). {3.2, Box 3.1}

- It is *about as likely as not* that ocean heat content from 0–700 m increased more slowly during 2003 to 2010 than during 1993 to 2002 (see Figure SPM.3). Ocean heat uptake from 700–2000 m, where interannual variability is smaller, *likely* continued unabated from 1993 to 2009. {3.2, Box 9.2}

- It is *very likely* that regions of high salinity where evaporation dominates have become more saline, while regions of low salinity where precipitation dominates have become fresher since the 1950s. These regional trends in ocean salinity provide indirect evidence that evaporation and precipitation over the oceans have changed (*medium confidence*). {2.5, 3.3, 3.5}

- There is no observational evidence of a trend in the Atlantic Meridional Overturning Circulation (AMOC), based on the decade-long record of the complete AMOC and longer records of individual AMOC components. {3.6}

[7] A constant supply of heat through the ocean surface at the rate of 1 W m^{-2} for 1 year would increase the ocean heat content by 1.1 × 10^{22} J.

B.3 Cryosphere

Over the last two decades, the Greenland and Antarctic ice sheets have been losing mass, glaciers have continued to shrink almost worldwide, and Arctic sea ice and Northern Hemisphere spring snow cover have continued to decrease in extent (*high confidence*) (see Figure SPM.3). {4.2–4.7}

- The average rate of ice loss[8] from glaciers around the world, excluding glaciers on the periphery of the ice sheets[9], was *very likely* 226 [91 to 361] Gt yr^{-1} over the period 1971 to 2009, and *very likely* 275 [140 to 410] Gt yr^{-1} over the period 1993 to 2009[10]. {4.3}

- The average rate of ice loss from the Greenland ice sheet has *very likely* substantially increased from 34 [–6 to 74] Gt yr^{-1} over the period 1992 to 2001 to 215 [157 to 274] Gt yr^{-1} over the period 2002 to 2011. {4.4}

- The average rate of ice loss from the Antarctic ice sheet has *likely* increased from 30 [–37 to 97] Gt yr^{-1} over the period 1992–2001 to 147 [72 to 221] Gt yr^{-1} over the period 2002 to 2011. There is *very high confidence* that these losses are mainly from the northern Antarctic Peninsula and the Amundsen Sea sector of West Antarctica. {4.4}

- The annual mean Arctic sea ice extent decreased over the period 1979 to 2012 with a rate that was *very likely* in the range 3.5 to 4.1% per decade (range of 0.45 to 0.51 million km^2 per decade), and *very likely* in the range 9.4 to 13.6% per decade (range of 0.73 to 1.07 million km^2 per decade) for the summer sea ice minimum (perennial sea ice). The average decrease in decadal mean extent of Arctic sea ice has been most rapid in summer (*high confidence*); the spatial extent has decreased in every season, and in every successive decade since 1979 (*high confidence*) (see Figure SPM.3). There is *medium confidence* from reconstructions that over the past three decades, Arctic summer sea ice retreat was unprecedented and sea surface temperatures were anomalously high in at least the last 1,450 years. {4.2, 5.5}

- It is *very likely* that the annual mean Antarctic sea ice extent increased at a rate in the range of 1.2 to 1.8% per decade (range of 0.13 to 0.20 million km^2 per decade) between 1979 and 2012. There is *high confidence* that there are strong regional differences in this annual rate, with extent increasing in some regions and decreasing in others. {4.2}

- There is *very high confidence* that the extent of Northern Hemisphere snow cover has decreased since the mid-20th century (see Figure SPM.3). Northern Hemisphere snow cover extent decreased 1.6 [0.8 to 2.4] % per decade for March and April, and 11.7 [8.8 to 14.6] % per decade for June, over the 1967 to 2012 period. During this period, snow cover extent in the Northern Hemisphere did not show a statistically significant increase in any month. {4.5}

- There is *high confidence* that permafrost temperatures have increased in most regions since the early 1980s. Observed warming was up to 3°C in parts of Northern Alaska (early 1980s to mid-2000s) and up to 2°C in parts of the Russian European North (1971 to 2010). In the latter region, a considerable reduction in permafrost thickness and areal extent has been observed over the period 1975 to 2005 (*medium confidence*). {4.7}

- Multiple lines of evidence support very substantial Arctic warming since the mid-20th century. {Box 5.1, 10.3}

---

[8] All references to 'ice loss' or 'mass loss' refer to net ice loss, i.e., accumulation minus melt and iceberg calving.

[9] For methodological reasons, this assessment of ice loss from the Antarctic and Greenland ice sheets includes change in the glaciers on the periphery. These peripheral glaciers are thus excluded from the values given for glaciers.

[10] 100 Gt yr^{-1} of ice loss is equivalent to about 0.28 mm yr^{-1} of global mean sea level rise.

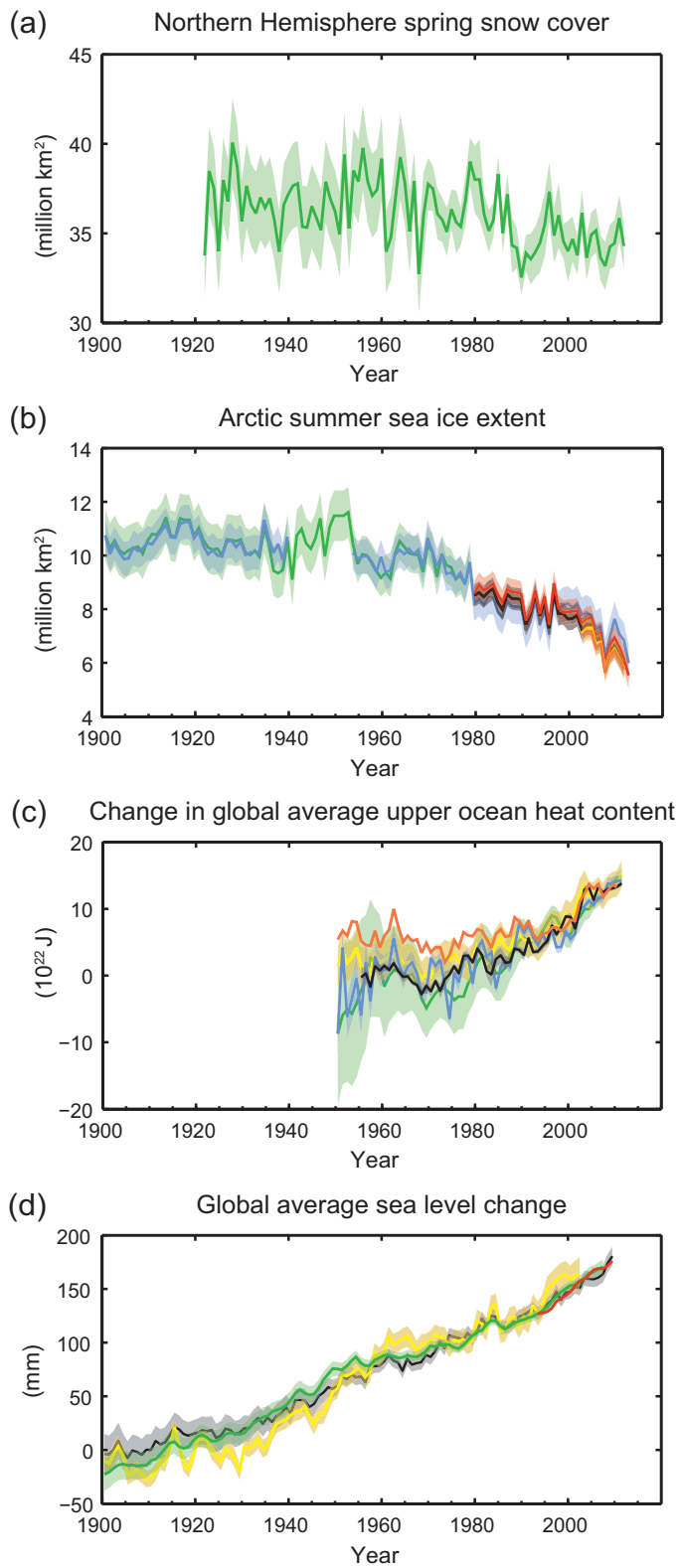

Figure SPM.3 | Multiple observed indicators of a changing global climate: (a) Extent of Northern Hemisphere March-April (spring) average snow cover; (b) extent of Arctic July-August-September (summer) average sea ice; (c) change in global mean upper ocean (0–700 m) heat content aligned to 2006–2010, and relative to the mean of all datasets for 1970; (d) global mean sea level relative to the 1900–1905 mean of the longest running dataset, and with all datasets aligned to have the same value in 1993, the first year of satellite altimetry data. All time-series (coloured lines indicating different data sets) show annual values, and where assessed, uncertainties are indicated by coloured shading. See Technical Summary Supplementary Material for a listing of the datasets. {Figures 3.2, 3.13, 4.19, and 4.3; FAQ 2.1, Figure 2; Figure TS.1}

B.4 Sea Level

The rate of sea level rise since the mid-19th century has been larger than the mean rate during the previous two millennia (*high confidence*). Over the period 1901 to 2010, global mean sea level rose by 0.19 [0.17 to 0.21] m (see Figure SPM.3). {3.7, 5.6, 13.2}

- Proxy and instrumental sea level data indicate a transition in the late 19th to the early 20th century from relatively low mean rates of rise over the previous two millennia to higher rates of rise (*high confidence*). It is *likely* that the rate of global mean sea level rise has continued to increase since the early 20th century. {3.7, 5.6, 13.2}

- It is *very likely* that the mean rate of global averaged sea level rise was 1.7 [1.5 to 1.9] mm yr^{-1} between 1901 and 2010, 2.0 [1.7 to 2.3] mm yr^{-1} between 1971 and 2010, and 3.2 [2.8 to 3.6] mm yr^{-1} between 1993 and 2010. Tide-gauge and satellite altimeter data are consistent regarding the higher rate of the latter period. It is *likely* that similarly high rates occurred between 1920 and 1950. {3.7}

- Since the early 1970s, glacier mass loss and ocean thermal expansion from warming together explain about 75% of the observed global mean sea level rise (*high confidence*). Over the period 1993 to 2010, global mean sea level rise is, with *high confidence*, consistent with the sum of the observed contributions from ocean thermal expansion due to warming (1.1 [0.8 to 1.4] mm yr^{-1}), from changes in glaciers (0.76 [0.39 to 1.13] mm yr^{-1}), Greenland ice sheet (0.33 [0.25 to 0.41] mm yr^{-1}), Antarctic ice sheet (0.27 [0.16 to 0.38] mm yr^{-1}), and land water storage (0.38 [0.26 to 0.49] mm yr^{-1}). The sum of these contributions is 2.8 [2.3 to 3.4] mm yr^{-1}. {13.3}

- There is *very high confidence* that maximum global mean sea level during the last interglacial period (129,000 to 116,000 years ago) was, for several thousand years, at least 5 m higher than present, and *high confidence* that it did not exceed 10 m above present. During the last interglacial period, the Greenland ice sheet *very likely* contributed between 1.4 and 4.3 m to the higher global mean sea level, implying with *medium confidence* an additional contribution from the Antarctic ice sheet. This change in sea level occurred in the context of different orbital forcing and with high-latitude surface temperature, averaged over several thousand years, at least 2°C warmer than present (*high confidence*). {5.3, 5.6}

B.5 Carbon and Other Biogeochemical Cycles

The atmospheric concentrations of carbon dioxide, methane, and nitrous oxide have increased to levels unprecedented in at least the last 800,000 years. Carbon dioxide concentrations have increased by 40% since pre-industrial times, primarily from fossil fuel emissions and secondarily from net land use change emissions. The ocean has absorbed about 30% of the emitted anthropogenic carbon dioxide, causing ocean acidification (see Figure SPM.4). {2.2, 3.8, 5.2, 6.2, 6.3}

- The atmospheric concentrations of the greenhouse gases carbon dioxide (CO_2), methane (CH_4), and nitrous oxide (N_2O) have all increased since 1750 due to human activity. In 2011 the concentrations of these greenhouse gases were 391 ppm[11], 1803 ppb, and 324 ppb, and exceeded the pre-industrial levels by about 40%, 150%, and 20%, respectively. {2.2, 5.2, 6.1, 6.2}

- Concentrations of CO_2, CH_4, and N_2O now substantially exceed the highest concentrations recorded in ice cores during the past 800,000 years. The mean rates of increase in atmospheric concentrations over the past century are, with *very high confidence*, unprecedented in the last 22,000 years. {5.2, 6.1, 6.2}

[11] ppm (parts per million) or ppb (parts per billion, 1 billion = 1,000 million) is the ratio of the number of gas molecules to the total number of molecules of dry air. For example, 300 ppm means 300 molecules of a gas per million molecules of dry air.

- Annual CO_2 emissions from fossil fuel combustion and cement production were 8.3 [7.6 to 9.0] GtC[12] yr^{-1} averaged over 2002–2011 (*high confidence*) and were 9.5 [8.7 to 10.3] GtC yr^{-1} in 2011, 54% above the 1990 level. Annual net CO_2 emissions from anthropogenic land use change were 0.9 [0.1 to 1.7] GtC yr^{-1} on average during 2002 to 2011 (*medium confidence*). {6.3}

- From 1750 to 2011, CO_2 emissions from fossil fuel combustion and cement production have released 375 [345 to 405] GtC to the atmosphere, while deforestation and other land use change are estimated to have released 180 [100 to 260] GtC. This results in cumulative anthropogenic emissions of 555 [470 to 640] GtC. {6.3}

- Of these cumulative anthropogenic CO_2 emissions, 240 [230 to 250] GtC have accumulated in the atmosphere, 155 [125 to 185] GtC have been taken up by the ocean and 160 [70 to 250] GtC have accumulated in natural terrestrial ecosystems (i.e., the cumulative residual land sink). {Figure TS.4, 3.8, 6.3}

- Ocean acidification is quantified by decreases in pH[13]. The pH of ocean surface water has decreased by 0.1 since the beginning of the industrial era (*high confidence*), corresponding to a 26% increase in hydrogen ion concentration (see Figure SPM.4). {3.8, Box 3.2}

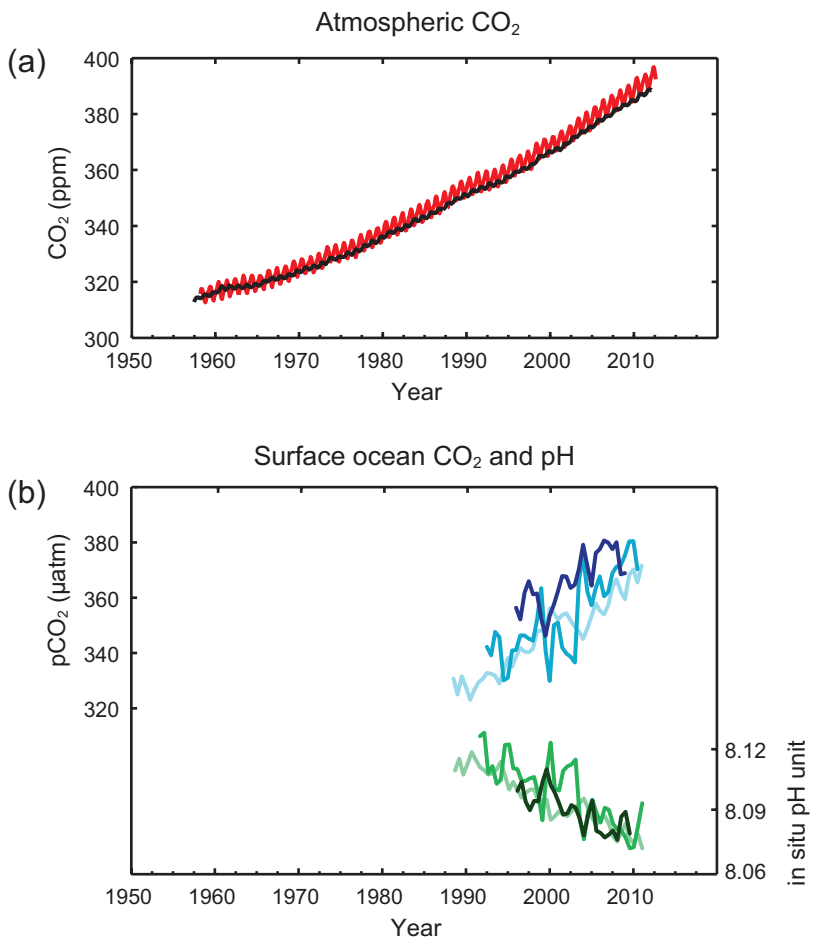

Figure SPM.4 | Multiple observed indicators of a changing global carbon cycle: (a) atmospheric concentrations of carbon dioxide (CO_2) from Mauna Loa (19°32′N, 155°34′W – red) and South Pole (89°59′S, 24°48′W – black) since 1958; (b) partial pressure of dissolved CO_2 at the ocean surface (blue curves) and in situ pH (green curves), a measure of the acidity of ocean water. Measurements are from three stations from the Atlantic (29°10′N, 15°30′W – dark blue/dark green; 31°40′N, 64°10′W – blue/green) and the Pacific Oceans (22°45′N, 158°00′W – light blue/light green). Full details of the datasets shown here are provided in the underlying report and the Technical Summary Supplementary Material. {Figures 2.1 and 3.18; Figure TS.5}

---

[12] 1 Gigatonne of carbon = 1 GtC = 10^{15} grams of carbon. This corresponds to 3.667 $GtCO_2$.

[13] pH is a measure of acidity using a logarithmic scale: a pH decrease of 1 unit corresponds to a 10-fold increase in hydrogen ion concentration, or acidity.

C. Drivers of Climate Change

Natural and anthropogenic substances and processes that alter the Earth's energy budget are drivers of climate change. Radiative forcing[14] (RF) quantifies the change in energy fluxes caused by changes in these drivers for 2011 relative to 1750, unless otherwise indicated. Positive RF leads to surface warming, negative RF leads to surface cooling. RF is estimated based on in-situ and remote observations, properties of greenhouse gases and aerosols, and calculations using numerical models representing observed processes. Some emitted compounds affect the atmospheric concentration of other substances. The RF can be reported based on the concentration changes of each substance[15]. Alternatively, the emission-based RF of a compound can be reported, which provides a more direct link to human activities. It includes contributions from all substances affected by that emission. The total anthropogenic RF of the two approaches are identical when considering all drivers. Though both approaches are used in this Summary for Policymakers, emission-based RFs are emphasized.

Total radiative forcing is positive, and has led to an uptake of energy by the climate system. The largest contribution to total radiative forcing is caused by the increase in the atmospheric concentration of CO_2 since 1750 (see Figure SPM.5). {3.2, Box 3.1, 8.3, 8.5}

- The total anthropogenic RF for 2011 relative to 1750 is 2.29 [1.13 to 3.33] W m^{-2} (see Figure SPM.5), and it has increased more rapidly since 1970 than during prior decades. The total anthropogenic RF best estimate for 2011 is 43% higher than that reported in AR4 for the year 2005. This is caused by a combination of continued growth in most greenhouse gas concentrations and improved estimates of RF by aerosols indicating a weaker net cooling effect (negative RF). {8.5}

- The RF from emissions of well-mixed greenhouse gases (CO_2, CH_4, N_2O, and Halocarbons) for 2011 relative to 1750 is 3.00 [2.22 to 3.78] W m^{-2} (see Figure SPM.5). The RF from changes in concentrations in these gases is 2.83 [2.26 to 3.40] W m^{-2}. {8.5}

- Emissions of CO_2 alone have caused an RF of 1.68 [1.33 to 2.03] W m^{-2} (see Figure SPM.5). Including emissions of other carbon-containing gases, which also contributed to the increase in CO_2 concentrations, the RF of CO_2 is 1.82 [1.46 to 2.18] W m^{-2}. {8.3, 8.5}

- Emissions of CH_4 alone have caused an RF of 0.97 [0.74 to 1.20] W m^{-2} (see Figure SPM.5). This is much larger than the concentration-based estimate of 0.48 [0.38 to 0.58] W m^{-2} (unchanged from AR4). This difference in estimates is caused by concentration changes in ozone and stratospheric water vapour due to CH_4 emissions and other emissions indirectly affecting CH_4. {8.3, 8.5}

- Emissions of stratospheric ozone-depleting halocarbons have caused a net positive RF of 0.18 [0.01 to 0.35] W m^{-2} (see Figure SPM.5). Their own positive RF has outweighed the negative RF from the ozone depletion that they have induced. The positive RF from all halocarbons is similar to the value in AR4, with a reduced RF from CFCs but increases from many of their substitutes. {8.3, 8.5}

- Emissions of short-lived gases contribute to the total anthropogenic RF. Emissions of carbon monoxide (CO) are *virtually certain* to have induced a positive RF, while emissions of nitrogen oxides (NO_x) are *likely* to have induced a net negative RF (see Figure SPM.5). {8.3, 8.5}

- The RF of the total aerosol effect in the atmosphere, which includes cloud adjustments due to aerosols, is –0.9 [–1.9 to –0.1] W m^{-2} (*medium confidence*), and results from a negative forcing from most aerosols and a positive contribution

[14] The strength of drivers is quantified as Radiative Forcing (RF) in units watts per square metre (W m^{-2}) as in previous IPCC assessments. RF is the change in energy flux caused by a driver, and is calculated at the tropopause or at the top of the atmosphere. In the traditional RF concept employed in previous IPCC reports all surface and tropospheric conditions are kept fixed. In calculations of RF for well-mixed greenhouse gases and aerosols in this report, physical variables, except for the ocean and sea ice, are allowed to respond to perturbations with rapid adjustments. The resulting forcing is called Effective Radiative Forcing (ERF) in the underlying report. This change reflects the scientific progress from previous assessments and results in a better indication of the eventual temperature response for these drivers. For all drivers other than well-mixed greenhouse gases and aerosols, rapid adjustments are less well characterized and assumed to be small, and thus the traditional RF is used. {8.1}

[15] This approach was used to report RF in the AR4 Summary for Policymakers.

from black carbon absorption of solar radiation. There is *high confidence* that aerosols and their interactions with clouds have offset a substantial portion of global mean forcing from well-mixed greenhouse gases. They continue to contribute the largest uncertainty to the total RF estimate. {7.5, 8.3, 8.5}

- The forcing from stratospheric volcanic aerosols can have a large impact on the climate for some years after volcanic eruptions. Several small eruptions have caused an RF of –0.11 [–0.15 to –0.08] W m^{-2} for the years 2008 to 2011, which is approximately twice as strong as during the years 1999 to 2002. {8.4}

- The RF due to changes in solar irradiance is estimated as 0.05 [0.00 to 0.10] W m^{-2} (see Figure SPM.5). Satellite observations of total solar irradiance changes from 1978 to 2011 indicate that the last solar minimum was lower than the previous two. This results in an RF of –0.04 [–0.08 to 0.00] W m^{-2} between the most recent minimum in 2008 and the 1986 minimum. {8.4}

- The total natural RF from solar irradiance changes and stratospheric volcanic aerosols made only a small contribution to the net radiative forcing throughout the last century, except for brief periods after large volcanic eruptions. {8.5}

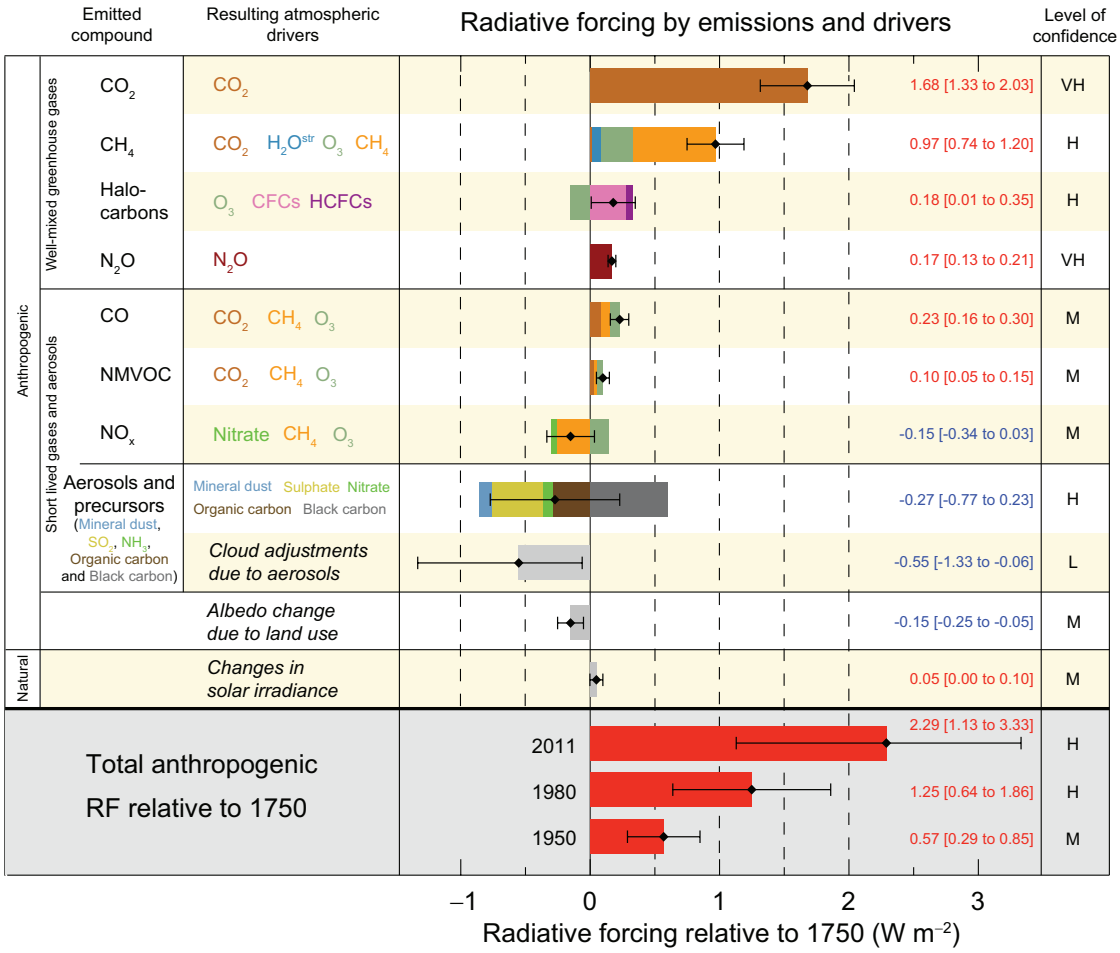

Figure SPM.5 | Radiative forcing estimates in 2011 relative to 1750 and aggregated uncertainties for the main drivers of climate change. Values are global average radiative forcing (RF[14]), partitioned according to the emitted compounds or processes that result in a combination of drivers. The best estimates of the net radiative forcing are shown as black diamonds with corresponding uncertainty intervals; the numerical values are provided on the right of the figure, together with the confidence level in the net forcing (VH – *very high*, H – *high*, M – *medium*, L – *low*, VL – *very low*). Albedo forcing due to black carbon on snow and ice is included in the black carbon aerosol bar. Small forcings due to contrails (0.05 W m^{-2}, including contrail induced cirrus), and HFCs, PFCs and SF_6 (total 0.03 W m^{-2}) are not shown. Concentration-based RFs for gases can be obtained by summing the like-coloured bars. Volcanic forcing is not included as its episodic nature makes is difficult to compare to other forcing mechanisms. Total anthropogenic radiative forcing is provided for three different years relative to 1750. For further technical details, including uncertainty ranges associated with individual components and processes, see the Technical Summary Supplementary Material. {8.5; Figures 8.14–8.18; Figures TS.6 and TS.7}

D. Understanding the Climate System and its Recent Changes

Understanding recent changes in the climate system results from combining observations, studies of feedback processes, and model simulations. Evaluation of the ability of climate models to simulate recent changes requires consideration of the state of all modelled climate system components at the start of the simulation and the natural and anthropogenic forcing used to drive the models. Compared to AR4, more detailed and longer observations and improved climate models now enable the attribution of a human contribution to detected changes in more climate system components.

Human influence on the climate system is clear. This is evident from the increasing greenhouse gas concentrations in the atmosphere, positive radiative forcing, observed warming, and understanding of the climate system. {2–14}

D.1 Evaluation of Climate Models

Climate models have improved since the AR4. Models reproduce observed continental-scale surface temperature patterns and trends over many decades, including the more rapid warming since the mid-20th century and the cooling immediately following large volcanic eruptions (*very high confidence*). {9.4, 9.6, 9.8}

- The long-term climate model simulations show a trend in global-mean surface temperature from 1951 to 2012 that agrees with the observed trend (*very high confidence*). There are, however, differences between simulated and observed trends over periods as short as 10 to 15 years (e.g., 1998 to 2012). {9.4, Box 9.2}

- The observed reduction in surface warming trend over the period 1998 to 2012 as compared to the period 1951 to 2012, is due in roughly equal measure to a reduced trend in radiative forcing and a cooling contribution from natural internal variability, which includes a possible redistribution of heat within the ocean (*medium confidence*). The reduced trend in radiative forcing is primarily due to volcanic eruptions and the timing of the downward phase of the 11-year solar cycle. However, there is *low confidence* in quantifying the role of changes in radiative forcing in causing the reduced warming trend. There is *medium confidence* that natural internal decadal variability causes to a substantial degree the difference between observations and the simulations; the latter are not expected to reproduce the timing of natural internal variability. There may also be a contribution from forcing inadequacies and, in some models, an overestimate of the response to increasing greenhouse gas and other anthropogenic forcing (dominated by the effects of aerosols). {9.4, Box 9.2, 10.3, Box 10.2, 11.3}

- On regional scales, the confidence in model capability to simulate surface temperature is less than for the larger scales. However, there is *high confidence* that regional-scale surface temperature is better simulated than at the time of the AR4. {9.4, 9.6}

- There has been substantial progress in the assessment of extreme weather and climate events since AR4. Simulated global-mean trends in the frequency of extreme warm and cold days and nights over the second half of the 20th century are generally consistent with observations. {9.5}

- There has been some improvement in the simulation of continental-scale patterns of precipitation since the AR4. At regional scales, precipitation is not simulated as well, and the assessment is hampered by observational uncertainties. {9.4, 9.6}

- Some important climate phenomena are now better reproduced by models. There is *high confidence* that the statistics of monsoon and El Niño-Southern Oscillation (ENSO) based on multi-model simulations have improved since AR4. {9.5}

- Climate models now include more cloud and aerosol processes, and their interactions, than at the time of the AR4, but there remains *low confidence* in the representation and quantification of these processes in models. {7.3, 7.6, 9.4, 9.7}

- There is robust evidence that the downward trend in Arctic summer sea ice extent since 1979 is now reproduced by more models than at the time of the AR4, with about one-quarter of the models showing a trend as large as, or larger than, the trend in the observations. Most models simulate a small downward trend in Antarctic sea ice extent, albeit with large inter-model spread, in contrast to the small upward trend in observations. {9.4}

- Many models reproduce the observed changes in upper-ocean heat content (0–700 m) from 1961 to 2005 (*high confidence*), with the multi-model mean time series falling within the range of the available observational estimates for most of the period. {9.4}

- Climate models that include the carbon cycle (Earth System Models) simulate the global pattern of ocean-atmosphere CO_2 fluxes, with outgassing in the tropics and uptake in the mid and high latitudes. In the majority of these models the sizes of the simulated global land and ocean carbon sinks over the latter part of the 20th century are within the range of observational estimates. {9.4}

D.2 Quantification of Climate System Responses

Observational and model studies of temperature change, climate feedbacks and changes in the Earth's energy budget together provide confidence in the magnitude of global warming in response to past and future forcing. {Box 12.2, Box 13.1}

- The net feedback from the combined effect of changes in water vapour, and differences between atmospheric and surface warming is *extremely likely* positive and therefore amplifies changes in climate. The net radiative feedback due to all cloud types combined is *likely* positive. Uncertainty in the sign and magnitude of the cloud feedback is due primarily to continuing uncertainty in the impact of warming on low clouds. {7.2}

- The equilibrium climate sensitivity quantifies the response of the climate system to constant radiative forcing on multi-century time scales. It is defined as the change in global mean surface temperature at equilibrium that is caused by a doubling of the atmospheric CO_2 concentration. Equilibrium climate sensitivity is *likely* in the range 1.5°C to 4.5°C (*high confidence*), *extremely unlikely* less than 1°C (*high confidence*), and *very unlikely* greater than 6°C (*medium confidence*)[16]. The lower temperature limit of the assessed *likely* range is thus less than the 2°C in the AR4, but the upper limit is the same. This assessment reflects improved understanding, the extended temperature record in the atmosphere and ocean, and new estimates of radiative forcing. {TS TFE.6, Figure 1; Box 12.2}

- The rate and magnitude of global climate change is determined by radiative forcing, climate feedbacks and the storage of energy by the climate system. Estimates of these quantities for recent decades are consistent with the assessed *likely* range of the equilibrium climate sensitivity to within assessed uncertainties, providing strong evidence for our understanding of anthropogenic climate change. {Box 12.2, Box 13.1}

- The transient climate response quantifies the response of the climate system to an increasing radiative forcing on a decadal to century timescale. It is defined as the change in global mean surface temperature at the time when the atmospheric CO_2 concentration has doubled in a scenario of concentration increasing at 1% per year. The transient climate response is *likely* in the range of 1.0°C to 2.5°C (*high confidence*) and *extremely unlikely* greater than 3°C. {Box 12.2}

- A related quantity is the transient climate response to cumulative carbon emissions (TCRE). It quantifies the transient response of the climate system to cumulative carbon emissions (see Section E.8). TCRE is defined as the global mean

[16] No best estimate for equilibrium climate sensitivity can now be given because of a lack of agreement on values across assessed lines of evidence and studies.

surface temperature change per 1000 GtC emitted to the atmosphere. TCRE is *likely* in the range of 0.8°C to 2.5°C per 1000 GtC and applies for cumulative emissions up to about 2000 GtC until the time temperatures peak (see Figure SPM.10). {12.5, Box 12.2}

- Various metrics can be used to compare the contributions to climate change of emissions of different substances. The most appropriate metric and time horizon will depend on which aspects of climate change are considered most important to a particular application. No single metric can accurately compare all consequences of different emissions, and all have limitations and uncertainties. The Global Warming Potential is based on the cumulative radiative forcing over a particular time horizon, and the Global Temperature Change Potential is based on the change in global mean surface temperature at a chosen point in time. Updated values are provided in the underlying Report. {8.7}

D.3 Detection and Attribution of Climate Change

Human influence has been detected in warming of the atmosphere and the ocean, in changes in the global water cycle, in reductions in snow and ice, in global mean sea level rise, and in changes in some climate extremes (see Figure SPM.6 and Table SPM.1). This evidence for human influence has grown since AR4. It is *extremely likely* that human influence has been the dominant cause of the observed warming since the mid-20th century. {10.3–10.6, 10.9}

- It is *extremely likely* that more than half of the observed increase in global average surface temperature from 1951 to 2010 was caused by the anthropogenic increase in greenhouse gas concentrations and other anthropogenic forcings together. The best estimate of the human-induced contribution to warming is similar to the observed warming over this period. {10.3}

- Greenhouse gases contributed a global mean surface warming *likely* to be in the range of 0.5°C to 1.3°C over the period 1951 to 2010, with the contributions from other anthropogenic forcings, including the cooling effect of aerosols, *likely* to be in the range of –0.6°C to 0.1°C. The contribution from natural forcings is *likely* to be in the range of –0.1°C to 0.1°C, and from natural internal variability is *likely* to be in the range of –0.1°C to 0.1°C. Together these assessed contributions are consistent with the observed warming of approximately 0.6°C to 0.7°C over this period. {10.3}

- Over every continental region except Antarctica, anthropogenic forcings have *likely* made a substantial contribution to surface temperature increases since the mid-20th century (see Figure SPM.6). For Antarctica, large observational uncertainties result in *low confidence* that anthropogenic forcings have contributed to the observed warming averaged over available stations. It is *likely* that there has been an anthropogenic contribution to the very substantial Arctic warming since the mid-20th century. {2.4, 10.3}

- It is *very likely* that anthropogenic influence, particularly greenhouse gases and stratospheric ozone depletion, has led to a detectable observed pattern of tropospheric warming and a corresponding cooling in the lower stratosphere since 1961. {2.4, 9.4, 10.3}

- It is *very likely* that anthropogenic forcings have made a substantial contribution to increases in global upper ocean heat content (0–700 m) observed since the 1970s (see Figure SPM.6). There is evidence for human influence in some individual ocean basins. {3.2, 10.4}

- It is *likely* that anthropogenic influences have affected the global water cycle since 1960. Anthropogenic influences have contributed to observed increases in atmospheric moisture content in the atmosphere (*medium confidence*), to global-scale changes in precipitation patterns over land (*medium confidence*), to intensification of heavy precipitation over land regions where data are sufficient (*medium confidence*), and to changes in surface and sub-surface ocean salinity (*very likely*). {2.5, 2.6, 3.3, 7.6, 10.3, 10.4}

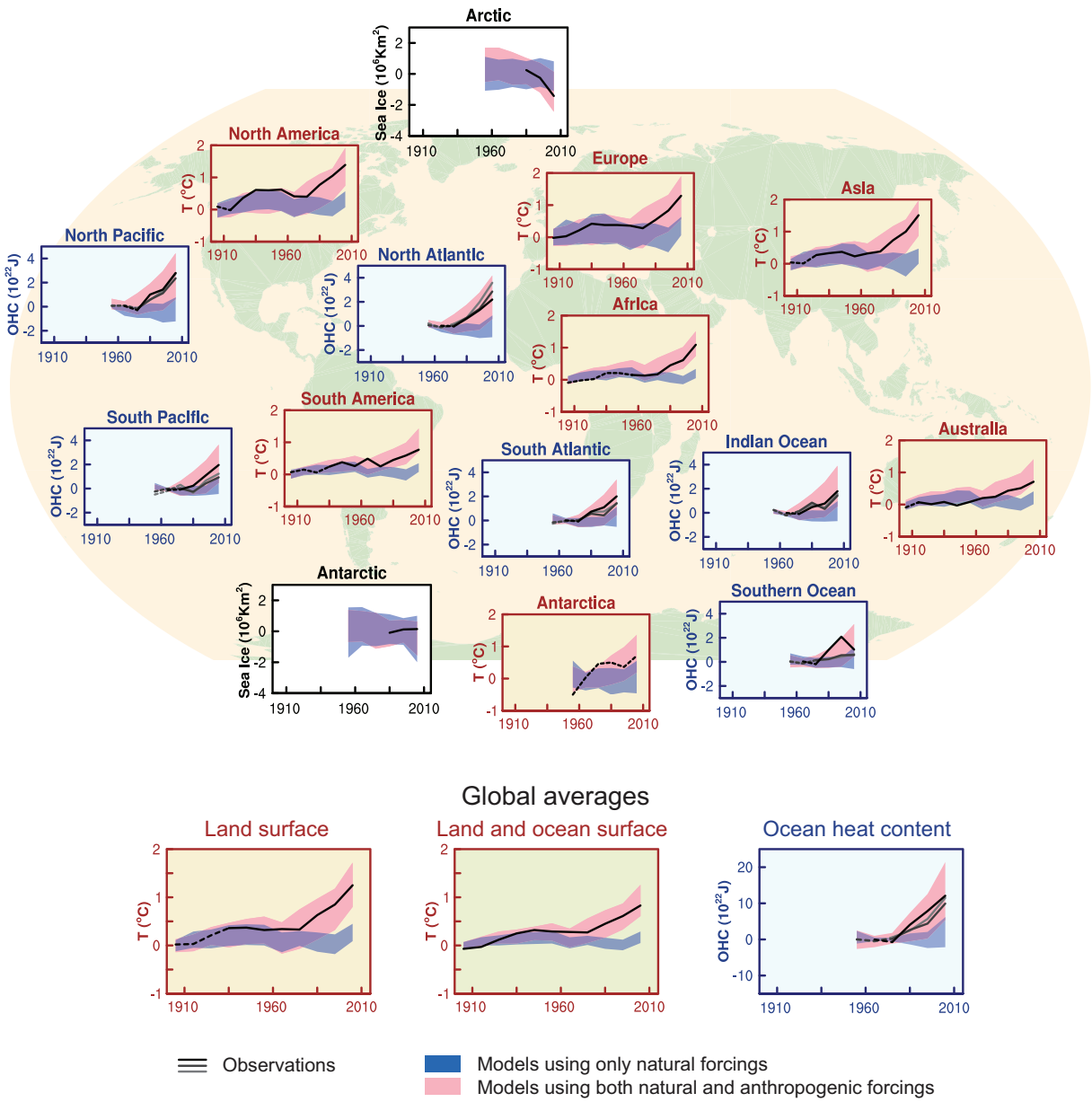

Figure SPM.6 | Comparison of observed and simulated climate change based on three large-scale indicators in the atmosphere, the cryosphere and the ocean: change in continental land surface air temperatures (yellow panels), Arctic and Antarctic September sea ice extent (white panels), and upper ocean heat content in the major ocean basins (blue panels). Global average changes are also given. Anomalies are given relative to 1880–1919 for surface temperatures, 1960–1980 for ocean heat content and 1979–1999 for sea ice. All time-series are decadal averages, plotted at the centre of the decade. For temperature panels, observations are dashed lines if the spatial coverage of areas being examined is below 50%. For ocean heat content and sea ice panels the solid line is where the coverage of data is good and higher in quality, and the dashed line is where the data coverage is only adequate, and thus, uncertainty is larger. Model results shown are Coupled Model Intercomparison Project Phase 5 (CMIP5) multi-model ensemble ranges, with shaded bands indicating the 5 to 95% confidence intervals. For further technical details, including region definitions see the Technical Summary Supplementary Material. {Figure 10.21; Figure TS.12}

- There has been further strengthening of the evidence for human influence on temperature extremes since the SREX. It is now *very likely* that human influence has contributed to observed global scale changes in the frequency and intensity of daily temperature extremes since the mid-20th century, and *likely* that human influence has more than doubled the probability of occurrence of heat waves in some locations (see Table SPM.1). {10.6}

- Anthropogenic influences have *very likely* contributed to Arctic sea ice loss since 1979. There is *low confidence* in the scientific understanding of the small observed increase in Antarctic sea ice extent due to the incomplete and competing scientific explanations for the causes of change and *low confidence* in estimates of natural internal variability in that region (see Figure SPM.6). {10.5}

- Anthropogenic influences *likely* contributed to the retreat of glaciers since the 1960s and to the increased surface mass loss of the Greenland ice sheet since 1993. Due to a low level of scientific understanding there is *low confidence* in attributing the causes of the observed loss of mass from the Antarctic ice sheet over the past two decades. {4.3, 10.5}

- It is *likely* that there has been an anthropogenic contribution to observed reductions in Northern Hemisphere spring snow cover since 1970. {10.5}

- It is *very likely* that there is a substantial anthropogenic contribution to the global mean sea level rise since the 1970s. This is based on the *high confidence* in an anthropogenic influence on the two largest contributions to sea level rise, that is thermal expansion and glacier mass loss. {10.4, 10.5, 13.3}

- There is *high confidence* that changes in total solar irradiance have not contributed to the increase in global mean surface temperature over the period 1986 to 2008, based on direct satellite measurements of total solar irradiance. There is *medium confidence* that the 11-year cycle of solar variability influences decadal climate fluctuations in some regions. No robust association between changes in cosmic rays and cloudiness has been identified. {7.4, 10.3, Box 10.2}

E. Future Global and Regional Climate Change

Projections of changes in the climate system are made using a hierarchy of climate models ranging from simple climate models, to models of intermediate complexity, to comprehensive climate models, and Earth System Models. These models simulate changes based on a set of scenarios of anthropogenic forcings. A new set of scenarios, the Representative Concentration Pathways (RCPs), was used for the new climate model simulations carried out under the framework of the Coupled Model Intercomparison Project Phase 5 (CMIP5) of the World Climate Research Programme. In all RCPs, atmospheric CO_2 concentrations are higher in 2100 relative to present day as a result of a further increase of cumulative emissions of CO_2 to the atmosphere during the 21st century (see Box SPM.1). Projections in this Summary for Policymakers are for the end of the 21st century (2081–2100) given relative to 1986–2005, unless otherwise stated. To place such projections in historical context, it is necessary to consider observed changes between different periods. Based on the longest global surface temperature dataset available, the observed change between the average of the period 1850–1900 and of the AR5 reference period is 0.61 [0.55 to 0.67] °C. However, warming has occurred beyond the average of the AR5 reference period. Hence this is not an estimate of historical warming to present (see Chapter 2) .

Continued emissions of greenhouse gases will cause further warming and changes in all components of the climate system. Limiting climate change will require substantial and sustained reductions of greenhouse gas emissions. {6, 11–14}

- Projections for the next few decades show spatial patterns of climate change similar to those projected for the later 21st century but with smaller magnitude. Natural internal variability will continue to be a major influence on climate, particularly in the near-term and at the regional scale. By the mid-21st century the magnitudes of the projected changes are substantially affected by the choice of emissions scenario (Box SPM.1). {11.3, Box 11.1, Annex I}

- Projected climate change based on RCPs is similar to AR4 in both patterns and magnitude, after accounting for scenario differences. The overall spread of projections for the high RCPs is narrower than for comparable scenarios used in AR4 because in contrast to the SRES emission scenarios used in AR4, the RCPs used in AR5 are defined as concentration pathways and thus carbon cycle uncertainties affecting atmospheric CO_2 concentrations are not considered in the concentration-driven CMIP5 simulations. Projections of sea level rise are larger than in the AR4, primarily because of improved modelling of land-ice contributions.{11.3, 12.3, 12.4, 13.4, 13.5}

E.1 Atmosphere: Temperature

Global surface temperature change for the end of the 21st century is *likely* to exceed 1.5°C relative to 1850 to 1900 for all RCP scenarios except RCP2.6. It is *likely* to exceed 2°C for RCP6.0 and RCP8.5, and *more likely than not* to exceed 2°C for RCP4.5. Warming will continue beyond 2100 under all RCP scenarios except RCP2.6. Warming will continue to exhibit interannual-to-decadal variability and will not be regionally uniform (see Figures SPM.7 and SPM.8). {11.3, 12.3, 12.4, 14.8}

- The global mean surface temperature change for the period 2016–2035 relative to 1986–2005 will *likely* be in the range of 0.3°C to 0.7°C (*medium confidence*). This assessment is based on multiple lines of evidence and assumes there will be no major volcanic eruptions or secular changes in total solar irradiance. Relative to natural internal variability, near-term increases in seasonal mean and annual mean temperatures are expected to be larger in the tropics and subtropics than in mid-latitudes (*high confidence*). {11.3}

- Increase of global mean surface temperatures for 2081–2100 relative to 1986–2005 is projected to *likely* be in the ranges derived from the concentration-driven CMIP5 model simulations, that is, 0.3°C to 1.7°C (RCP2.6), 1.1°C to 2.6°C (RCP4.5), 1.4°C to 3.1°C (RCP6.0), 2.6°C to 4.8°C (RCP8.5). The Arctic region will warm more rapidly than the global mean, and mean warming over land will be larger than over the ocean (*very high confidence*) (see Figures SPM.7 and SPM.8, and Table SPM.2). {12.4, 14.8}

- Relative to the average from year 1850 to 1900, global surface temperature change by the end of the 21st century is projected to *likely* exceed 1.5°C for RCP4.5, RCP6.0 and RCP8.5 (*high confidence*). Warming is *likely* to exceed 2°C for RCP6.0 and RCP8.5 (*high confidence*), *more likely than not* to exceed 2°C for RCP4.5 (*high confidence*), but *unlikely* to exceed 2°C for RCP2.6 (*medium confidence*). Warming is *unlikely* to exceed 4°C for RCP2.6, RCP4.5 and RCP6.0 (*high confidence*) and is *about as likely as not* to exceed 4°C for RCP8.5 (*medium confidence*). {12.4}

- It is *virtually certain* that there will be more frequent hot and fewer cold temperature extremes over most land areas on daily and seasonal timescales as global mean temperatures increase. It is *very likely* that heat waves will occur with a higher frequency and duration. Occasional cold winter extremes will continue to occur (see Table SPM.1). {12.4}

E.2 Atmosphere: Water Cycle

Changes in the global water cycle in response to the warming over the 21st century will not be uniform. The contrast in precipitation between wet and dry regions and between wet and dry seasons will increase, although there may be regional exceptions (see Figure SPM.8). {12.4, 14.3}

- Projected changes in the water cycle over the next few decades show similar large-scale patterns to those towards the end of the century, but with smaller magnitude. Changes in the near-term, and at the regional scale will be strongly influenced by natural internal variability and may be affected by anthropogenic aerosol emissions. {11.3}

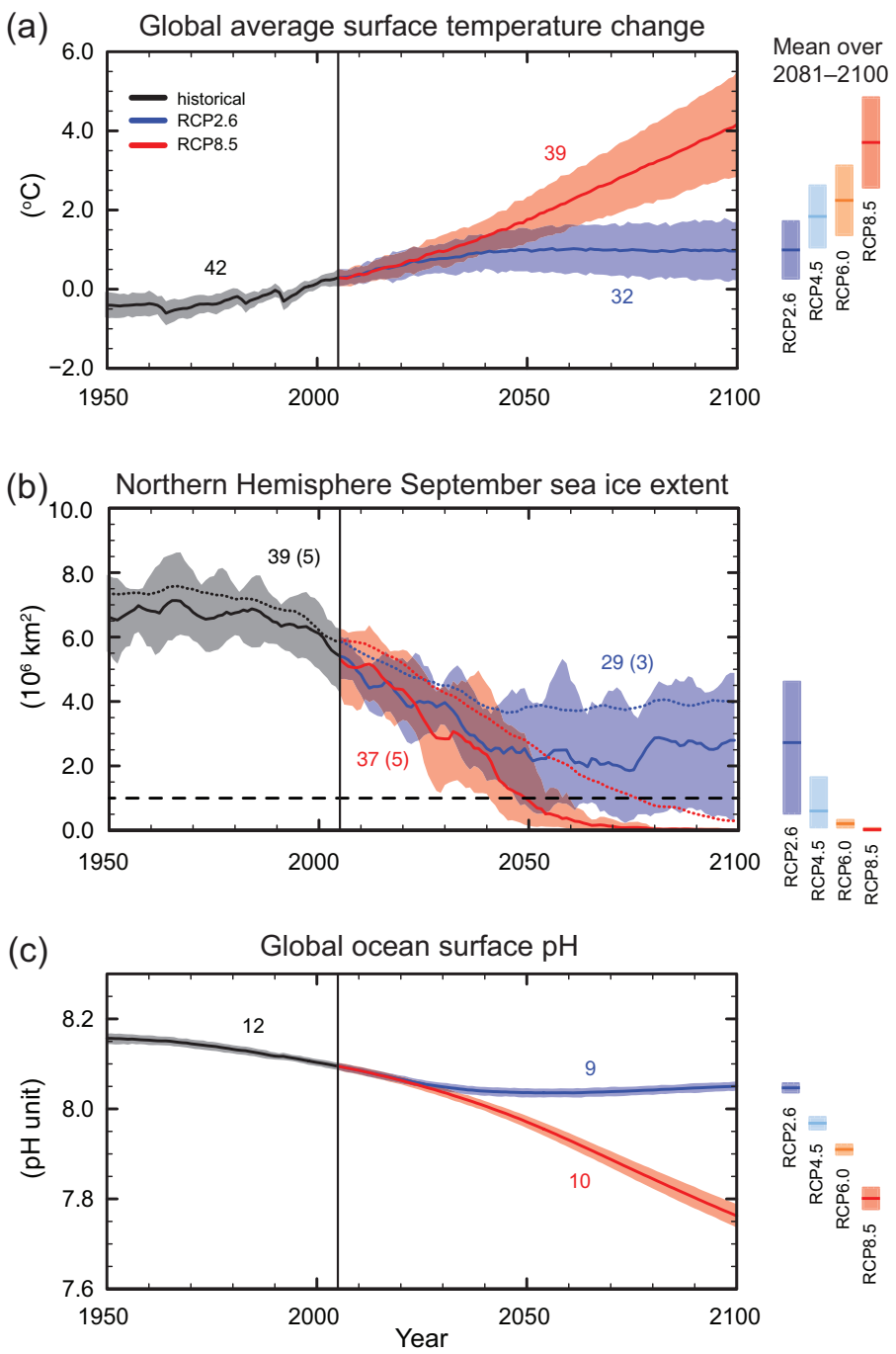

Figure SPM.7 | CMIP5 multi-model simulated time series from 1950 to 2100 for (a) change in global annual mean surface temperature relative to 1986–2005, (b) Northern Hemisphere September sea ice extent (5-year running mean), and (c) global mean ocean surface pH. Time series of projections and a measure of uncertainty (shading) are shown for scenarios RCP2.6 (blue) and RCP8.5 (red). Black (grey shading) is the modelled historical evolution using historical reconstructed forcings. The mean and associated uncertainties averaged over 2081–2100 are given for all RCP scenarios as colored vertical bars. The numbers of CMIP5 models used to calculate the multi-model mean is indicated. For sea ice extent (b), the projected mean and uncertainty (minimum-maximum range) of the subset of models that most closely reproduce the climatological mean state and 1979 to 2012 trend of the Arctic sea ice is given (number of models given in brackets). For completeness, the CMIP5 multi-model mean is also indicated with dotted lines. The dashed line represents nearly ice-free conditions (i.e., when sea ice extent is less than 10^6 km^2 for at least five consecutive years). For further technical details see the Technical Summary Supplementary Material {Figures 6.28, 12.5, and 12.28–12.31; Figures TS.15, TS.17, and TS.20}

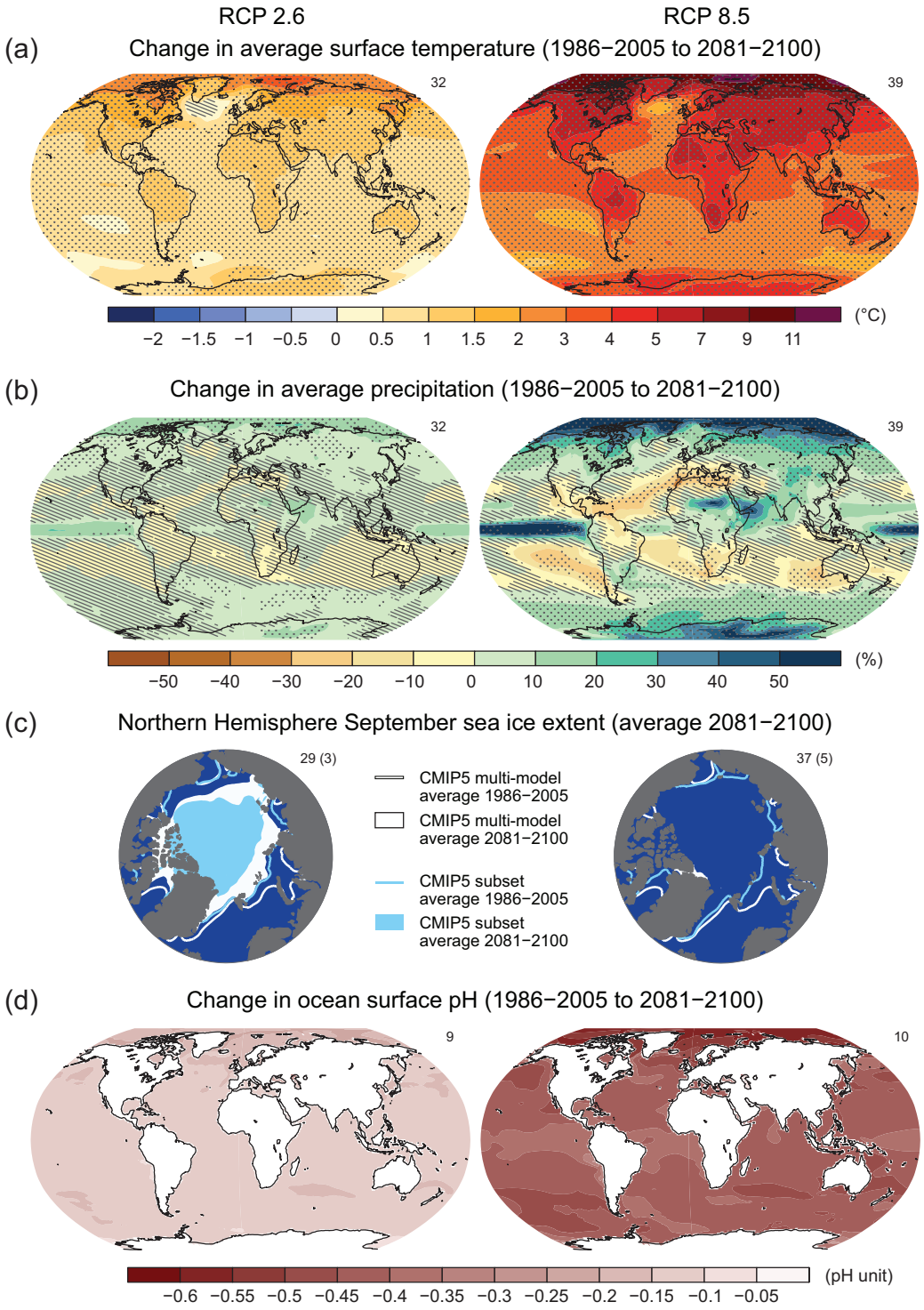

Figure SPM.8 | Maps of CMIP5 multi-model mean results for the scenarios RCP2.6 and RCP8.5 in 2081–2100 of (a) annual mean surface temperature change, (b) average percent change in annual mean precipitation, (c) Northern Hemisphere September sea ice extent, and (d) change in ocean surface pH. Changes in panels (a), (b) and (d) are shown relative to 1986–2005. The number of CMIP5 models used to calculate the multi-model mean is indicated in the upper right corner of each panel. For panels (a) and (b), hatching indicates regions where the multi-model mean is small compared to natural internal variability (i.e., less than one standard deviation of natural internal variability in 20-year means). Stippling indicates regions where the multi-model mean is large compared to natural internal variability (i.e., greater than two standard deviations of natural internal variability in 20-year means) and where at least 90% of models agree on the sign of change (see Box 12.1). In panel (c), the lines are the modelled means for 1986–2005; the filled areas are for the end of the century. The CMIP5 multi-model mean is given in white colour, the projected mean sea ice extent of a subset of models (number of models given in brackets) that most closely reproduce the climatological mean state and 1979 to 2012 trend of the Arctic sea ice extent is given in light blue colour. For further technical details see the Technical Summary Supplementary Material. {Figures 6.28, 12.11, 12.22, and 12.29; Figures TS.15, TS.16, TS.17, and TS.20}

- The high latitudes and the equatorial Pacific Ocean are *likely* to experience an increase in annual mean precipitation by the end of this century under the RCP8.5 scenario. In many mid-latitude and subtropical dry regions, mean precipitation will *likely* decrease, while in many mid-latitude wet regions, mean precipitation will *likely* increase by the end of this century under the RCP8.5 scenario (see Figure SPM.8). {7.6, 12.4, 14.3}

- Extreme precipitation events over most of the mid-latitude land masses and over wet tropical regions will *very likely* become more intense and more frequent by the end of this century, as global mean surface temperature increases (see Table SPM.1). {7.6, 12.4}

- Globally, it is *likely* that the area encompassed by monsoon systems will increase over the 21st century. While monsoon winds are *likely* to weaken, monsoon precipitation is *likely* to intensify due to the increase in atmospheric moisture. Monsoon onset dates are *likely* to become earlier or not to change much. Monsoon retreat dates will *likely* be delayed, resulting in lengthening of the monsoon season in many regions. {14.2}

- There is *high confidence* that the El Niño-Southern Oscillation (ENSO) will remain the dominant mode of interannual variability in the tropical Pacific, with global effects in the 21st century. Due to the increase in moisture availability, ENSO-related precipitation variability on regional scales will *likely* intensify. Natural variations of the amplitude and spatial pattern of ENSO are large and thus *confidence* in any specific projected change in ENSO and related regional phenomena for the 21st century remains *low*. {5.4, 14.4}

Table SPM.2 | Projected change in global mean surface air temperature and global mean sea level rise for the mid- and late 21st century relative to the reference period of 1986–2005. {12.4; Table 12.2, Table 13.5}

		2046–2065		2081–2100	
	Scenario	**Mean**	***Likely* range[c]**	**Mean**	***Likely* range[c]**
Global Mean Surface Temperature Change (°C)[a]	RCP2.6	1.0	0.4 to 1.6	1.0	0.3 to 1.7
	RCP4.5	1.4	0.9 to 2.0	1.8	1.1 to 2.6
	RCP6.0	1.3	0.8 to 1.8	2.2	1.4 to 3.1
	RCP8.5	2.0	1.4 to 2.6	3.7	2.6 to 4.8
	Scenario	**Mean**	***Likely* range[d]**	**Mean**	***Likely* range[d]**
Global Mean Sea Level Rise (m)[b]	RCP2.6	0.24	0.17 to 0.32	0.40	0.26 to 0.55
	RCP4.5	0.26	0.19 to 0.33	0.47	0.32 to 0.63
	RCP6.0	0.25	0.18 to 0.32	0.48	0.33 to 0.63
	RCP8.5	0.30	0.22 to 0.38	0.63	0.45 to 0.82

Notes:

[a] Based on the CMIP5 ensemble; anomalies calculated with respect to 1986–2005. Using HadCRUT4 and its uncertainty estimate (5–95% confidence interval), the observed warming to the reference period 1986–2005 is 0.61 [0.55 to 0.67] °C from 1850–1900, and 0.11 [0.09 to 0.13] °C from 1980–1999, the reference period for projections used in AR4. *Likely* ranges have not been assessed here with respect to earlier reference periods because methods are not generally available in the literature for combining the uncertainties in models and observations. Adding projected and observed changes does not account for potential effects of model biases compared to observations, and for natural internal variability during the observational reference period {2.4; 11.2; Tables 12.2 and 12.3}

[b] Based on 21 CMIP5 models; anomalies calculated with respect to 1986–2005. Where CMIP5 results were not available for a particular AOGCM and scenario, they were estimated as explained in Chapter 13, Table 13.5. The contributions from ice sheet rapid dynamical change and anthropogenic land water storage are treated as having uniform probability distributions, and as largely independent of scenario. This treatment does not imply that the contributions concerned will not depend on the scenario followed, only that the current state of knowledge does not permit a quantitative assessment of the dependence. Based on current understanding, only the collapse of marine-based sectors of the Antarctic ice sheet, if initiated, could cause global mean sea level to rise substantially above the *likely* range during the 21st century. There is *medium confidence* that this additional contribution would not exceed several tenths of a meter of sea level rise during the 21st century.

[c] Calculated from projections as 5–95% model ranges. These ranges are then assessed to be *likely* ranges after accounting for additional uncertainties or different levels of confidence in models. For projections of global mean surface temperature change in 2046–2065 *confidence* is *medium*, because the relative importance of natural internal variability, and uncertainty in non-greenhouse gas forcing and response, are larger than for 2081–2100. The *likely* ranges for 2046–2065 do not take into account the possible influence of factors that lead to the assessed range for near-term (2016–2035) global mean surface temperature change that is lower than the 5–95% model range, because the influence of these factors on longer term projections has not been quantified due to insufficient scientific understanding. {11.3}

[d] Calculated from projections as 5–95% model ranges. These ranges are then assessed to be *likely* ranges after accounting for additional uncertainties or different levels of confidence in models. For projections of global mean sea level rise *confidence* is *medium* for both time horizons.

E.3 Atmosphere: Air Quality

- The range in projections of air quality (ozone and PM2.5[17] in near-surface air) is driven primarily by emissions (including CH_4), rather than by physical climate change (*medium confidence*). There is *high confidence* that globally, warming decreases background surface ozone. High CH_4 levels (as in RCP8.5) can offset this decrease, raising background surface ozone by year 2100 on average by about 8 ppb (25% of current levels) relative to scenarios with small CH_4 changes (as in RCP4.5 and RCP6.0) (*high confidence*). {11.3}

- Observational and modelling evidence indicates that, all else being equal, locally higher surface temperatures in polluted regions will trigger regional feedbacks in chemistry and local emissions that will increase peak levels of ozone and PM2.5 (*medium confidence*). For PM2.5, climate change may alter natural aerosol sources as well as removal by precipitation, but no confidence level is attached to the overall impact of climate change on PM2.5 distributions. {11.3}

E.4 Ocean

The global ocean will continue to warm during the 21st century. Heat will penetrate from the surface to the deep ocean and affect ocean circulation. {11.3, 12.4}

- The strongest ocean warming is projected for the surface in tropical and Northern Hemisphere subtropical regions. At greater depth the warming will be most pronounced in the Southern Ocean (*high confidence*). Best estimates of ocean warming in the top one hundred meters are about 0.6°C (RCP2.6) to 2.0°C (RCP8.5), and about 0.3°C (RCP2.6) to 0.6°C (RCP8.5) at a depth of about 1000 m by the end of the 21st century. {12.4, 14.3}

- It is *very likely* that the Atlantic Meridional Overturning Circulation (AMOC) will weaken over the 21st century. Best estimates and ranges[18] for the reduction are 11% (1 to 24%) in RCP2.6 and 34% (12 to 54%) in RCP8.5. It is *likely* that there will be some decline in the AMOC by about 2050, but there may be some decades when the AMOC increases due to large natural internal variability. {11.3, 12.4}

- It is *very unlikely* that the AMOC will undergo an abrupt transition or collapse in the 21st century for the scenarios considered. There is *low confidence* in assessing the evolution of the AMOC beyond the 21st century because of the limited number of analyses and equivocal results. However, a collapse beyond the 21st century for large sustained warming cannot be excluded. {12.5}

E.5 Cryosphere

It is *very likely* that the Arctic sea ice cover will continue to shrink and thin and that Northern Hemisphere spring snow cover will decrease during the 21st century as global mean surface temperature rises. Global glacier volume will further decrease. {12.4, 13.4}

- Year-round reductions in Arctic sea ice extent are projected by the end of the 21st century from multi-model averages. These reductions range from 43% for RCP2.6 to 94% for RCP8.5 in September and from 8% for RCP2.6 to 34% for RCP8.5 in February (*medium confidence*) (see Figures SPM.7 and SPM.8). {12.4}

[17] PM2.5 refers to particulate matter with a diameter of less than 2.5 micrometres, a measure of atmospheric aerosol concentration.

[18] The ranges in this paragraph indicate a CMIP5 model spread.

- Based on an assessment of the subset of models that most closely reproduce the climatological mean state and 1979 to 2012 trend of the Arctic sea ice extent, a nearly ice-free Arctic Ocean[19] in September before mid-century is *likely* for RCP8.5 (*medium confidence*) (see Figures SPM.7 and SPM.8). A projection of when the Arctic might become nearly ice-free in September in the 21st century cannot be made with confidence for the other scenarios. {11.3, 12.4, 12.5}

- In the Antarctic, a decrease in sea ice extent and volume is projected with *low confidence* for the end of the 21st century as global mean surface temperature rises. {12.4}

- By the end of the 21st century, the global glacier volume, excluding glaciers on the periphery of Antarctica, is projected to decrease by 15 to 55% for RCP2.6, and by 35 to 85% for RCP8.5 (*medium confidence*). {13.4, 13.5}

- The area of Northern Hemisphere spring snow cover is projected to decrease by 7% for RCP2.6 and by 25% in RCP8.5 by the end of the 21st century for the model average (*medium confidence*). {12.4}

- It is *virtually certain* that near-surface permafrost extent at high northern latitudes will be reduced as global mean surface temperature increases. By the end of the 21st century, the area of permafrost near the surface (upper 3.5 m) is projected to decrease by between 37% (RCP2.6) to 81% (RCP8.5) for the model average (*medium confidence*). {12.4}

E.6 Sea Level

Global mean sea level will continue to rise during the 21st century (see Figure SPM.9). Under all RCP scenarios, the rate of sea level rise will *very likely* exceed that observed during 1971 to 2010 due to increased ocean warming and increased loss of mass from glaciers and ice sheets. {13.3–13.5}

- Confidence in projections of global mean sea level rise has increased since the AR4 because of the improved physical understanding of the components of sea level, the improved agreement of process-based models with observations, and the inclusion of ice-sheet dynamical changes. {13.3–13.5}

- Global mean sea level rise for 2081–2100 relative to 1986–2005 will *likely* be in the ranges of 0.26 to 0.55 m for RCP2.6, 0.32 to 0.63 m for RCP4.5, 0.33 to 0.63 m for RCP6.0, and 0.45 to 0.82 m for RCP8.5 (*medium confidence*). For RCP8.5, the rise by the year 2100 is 0.52 to 0.98 m, with a rate during 2081 to 2100 of 8 to 16 mm yr^{-1} (*medium confidence*). These ranges are derived from CMIP5 climate projections in combination with process-based models and literature assessment of glacier and ice sheet contributions (see Figure SPM.9, Table SPM.2). {13.5}

- In the RCP projections, thermal expansion accounts for 30 to 55% of 21st century global mean sea level rise, and glaciers for 15 to 35%. The increase in surface melting of the Greenland ice sheet will exceed the increase in snowfall, leading to a positive contribution from changes in surface mass balance to future sea level (*high confidence*). While surface melting will remain small, an increase in snowfall on the Antarctic ice sheet is expected (*medium confidence*), resulting in a negative contribution to future sea level from changes in surface mass balance. Changes in outflow from both ice sheets combined will *likely* make a contribution in the range of 0.03 to 0.20 m by 2081–2100 (*medium confidence*). {13.3–13.5}

- Based on current understanding, only the collapse of marine-based sectors of the Antarctic ice sheet, if initiated, could cause global mean sea level to rise substantially above the *likely* range during the 21st century. However, there is *medium confidence* that this additional contribution would not exceed several tenths of a meter of sea level rise during the 21st century. {13.4, 13.5}

[19] Conditions in the Arctic Ocean are referred to as nearly ice-free when the sea ice extent is less than 10^6 km^2 for at least five consecutive years.

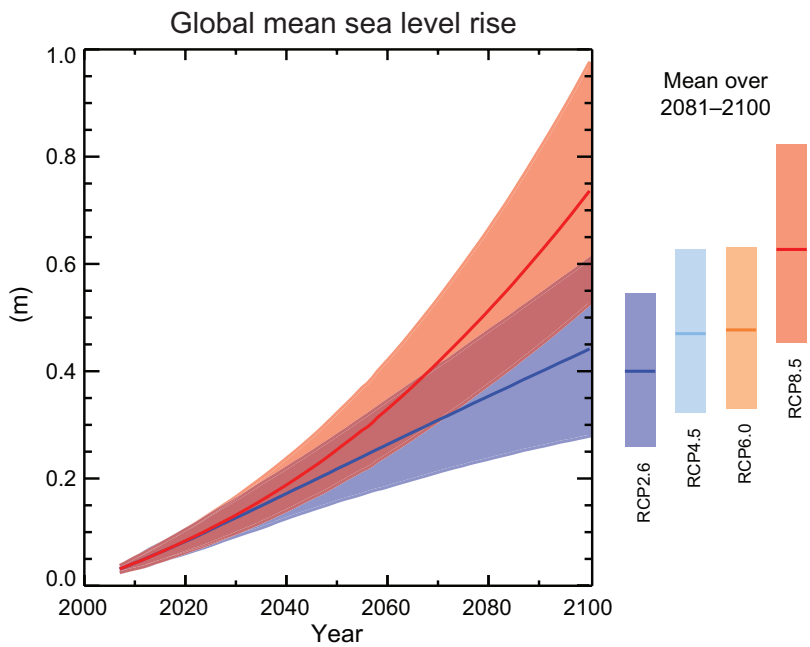

Figure SPM.9 | Projections of global mean sea level rise over the 21st century relative to 1986–2005 from the combination of the CMIP5 ensemble with process-based models, for RCP2.6 and RCP8.5. The assessed *likely* range is shown as a shaded band. The assessed *likely* ranges for the mean over the period 2081–2100 for all RCP scenarios are given as coloured vertical bars, with the corresponding median value given as a horizontal line. For further technical details see the Technical Summary Supplementary Material {Table 13.5, Figures 13.10 and 13.11; Figures TS.21 and TS.22}

- The basis for higher projections of global mean sea level rise in the 21st century has been considered and it has been concluded that there is currently insufficient evidence to evaluate the probability of specific levels above the assessed *likely* range. Many semi-empirical model projections of global mean sea level rise are higher than process-based model projections (up to about twice as large), but there is no consensus in the scientific community about their reliability and there is thus *low confidence* in their projections. {13.5}

- Sea level rise will not be uniform. By the end of the 21st century, it is *very likely* that sea level will rise in more than about 95% of the ocean area. About 70% of the coastlines worldwide are projected to experience sea level change within 20% of the global mean sea level change. {13.1, 13.6}

E.7 Carbon and Other Biogeochemical Cycles

Climate change will affect carbon cycle processes in a way that will exacerbate the increase of CO_2 in the atmosphere (*high confidence*). Further uptake of carbon by the ocean will increase ocean acidification. {6.4}

- Ocean uptake of anthropogenic CO_2 will continue under all four RCPs through to 2100, with higher uptake for higher concentration pathways (*very high confidence*). The future evolution of the land carbon uptake is less certain. A majority of models projects a continued land carbon uptake under all RCPs, but some models simulate a land carbon loss due to the combined effect of climate change and land use change. {6.4}

- Based on Earth System Models, there is *high confidence* that the feedback between climate and the carbon cycle is positive in the 21st century; that is, climate change will partially offset increases in land and ocean carbon sinks caused by rising atmospheric CO_2. As a result more of the emitted anthropogenic CO_2 will remain in the atmosphere. A positive feedback between climate and the carbon cycle on century to millennial time scales is supported by paleoclimate observations and modelling. {6.2, 6.4}

Table SPM.3 | Cumulative CO_2 emissions for the 2012 to 2100 period compatible with the RCP atmospheric concentrations simulated by the CMIP5 Earth System Models. {6.4, Table 6.12, Figure TS.19}

Scenario	Cumulative CO_2 Emissions 2012 to 2100[a]			
	GtC		$GtCO_2$	
	Mean	Range	Mean	Range
RCP2.6	270	140 to 410	990	510 to 1505
RCP4.5	780	595 to 1005	2860	2180 to 3690
RCP6.0	1060	840 to 1250	3885	3080 to 4585
RCP8.5	1685	1415 to 1910	6180	5185 to 7005

Notes:
[a] 1 Gigatonne of carbon = 1 GtC = 10^{15} grams of carbon. This corresponds to 3.667 $GtCO_2$.

- Earth System Models project a global increase in ocean acidification for all RCP scenarios. The corresponding decrease in surface ocean pH by the end of 21st century is in the range[18] of 0.06 to 0.07 for RCP2.6, 0.14 to 0.15 for RCP4.5, 0.20 to 0.21 for RCP6.0, and 0.30 to 0.32 for RCP8.5 (see Figures SPM.7 and SPM.8). {6.4}

- Cumulative CO_2 emissions[20] for the 2012 to 2100 period compatible with the RCP atmospheric CO_2 concentrations, as derived from 15 Earth System Models, range[18] from 140 to 410 GtC for RCP2.6, 595 to 1005 GtC for RCP4.5, 840 to 1250 GtC for RCP6.0, and 1415 to 1910 GtC for RCP8.5 (see Table SPM.3). {6.4}

- By 2050, annual CO_2 emissions derived from Earth System Models following RCP2.6 are smaller than 1990 emissions (by 14 to 96%). By the end of the 21st century, about half of the models infer emissions slightly above zero, while the other half infer a net removal of CO_2 from the atmosphere. {6.4, Figure TS.19}

- The release of CO_2 or CH_4 to the atmosphere from thawing permafrost carbon stocks over the 21st century is assessed to be in the range of 50 to 250 GtC for RCP8.5 (*low confidence*). {6.4}

E.8 Climate Stabilization, Climate Change Commitment and Irreversibility

Cumulative emissions of CO_2 largely determine global mean surface warming by the late 21st century and beyond (see Figure SPM.10). Most aspects of climate change will persist for many centuries even if emissions of CO_2 are stopped. This represents a substantial multi-century climate change commitment created by past, present and future emissions of CO_2. {12.5}

- Cumulative total emissions of CO_2 and global mean surface temperature response are approximately linearly related (see Figure SPM.10). Any given level of warming is associated with a range of cumulative CO_2 emissions[21], and therefore, e.g., higher emissions in earlier decades imply lower emissions later. {12.5}

- Limiting the warming caused by anthropogenic CO_2 emissions alone with a probability of >33%, >50%, and >66% to less than 2°C since the period 1861–1880[22], will require cumulative CO_2 emissions from all anthropogenic sources to stay between 0 and about 1570 GtC (5760 $GtCO_2$), 0 and about 1210 GtC (4440 $GtCO_2$), and 0 and about 1000 GtC (3670 $GtCO_2$) since that period, respectively[23]. These upper amounts are reduced to about 900 GtC (3300 $GtCO_2$), 820 GtC (3010 $GtCO_2$), and 790 GtC (2900 $GtCO_2$), respectively, when accounting for non-CO_2 forcings as in RCP2.6. An amount of 515 [445 to 585] GtC (1890 [1630 to 2150] $GtCO_2$), was already emitted by 2011. {12.5}

[20] From fossil fuel, cement, industry, and waste sectors.

[21] Quantification of this range of CO_2 emissions requires taking into account non-CO_2 drivers.

[22] The first 20-year period available from the models.

[23] This is based on the assessment of the transient climate response to cumulative carbon emissions (TCRE, see Section D.2).

- A lower warming target, or a higher likelihood of remaining below a specific warming target, will require lower cumulative CO_2 emissions. Accounting for warming effects of increases in non-CO_2 greenhouse gases, reductions in aerosols, or the release of greenhouse gases from permafrost will also lower the cumulative CO_2 emissions for a specific warming target (see Figure SPM.10). {12.5}

- A large fraction of anthropogenic climate change resulting from CO_2 emissions is irreversible on a multi-century to millennial time scale, except in the case of a large net removal of CO_2 from the atmosphere over a sustained period. Surface temperatures will remain approximately constant at elevated levels for many centuries after a complete cessation of net anthropogenic CO_2 emissions. Due to the long time scales of heat transfer from the ocean surface to depth, ocean warming will continue for centuries. Depending on the scenario, about 15 to 40% of emitted CO_2 will remain in the atmosphere longer than 1,000 years. {Box 6.1, 12.4, 12.5}

- It is *virtually certain* that global mean sea level rise will continue beyond 2100, with sea level rise due to thermal expansion to continue for many centuries. The few available model results that go beyond 2100 indicate global mean sea level rise above the pre-industrial level by 2300 to be less than 1 m for a radiative forcing that corresponds to CO_2 concentrations that peak and decline and remain below 500 ppm, as in the scenario RCP2.6. For a radiative forcing that corresponds to a CO_2 concentration that is above 700 ppm but below 1500 ppm, as in the scenario RCP8.5, the projected rise is 1 m to more than 3 m (*medium confidence*). {13.5}

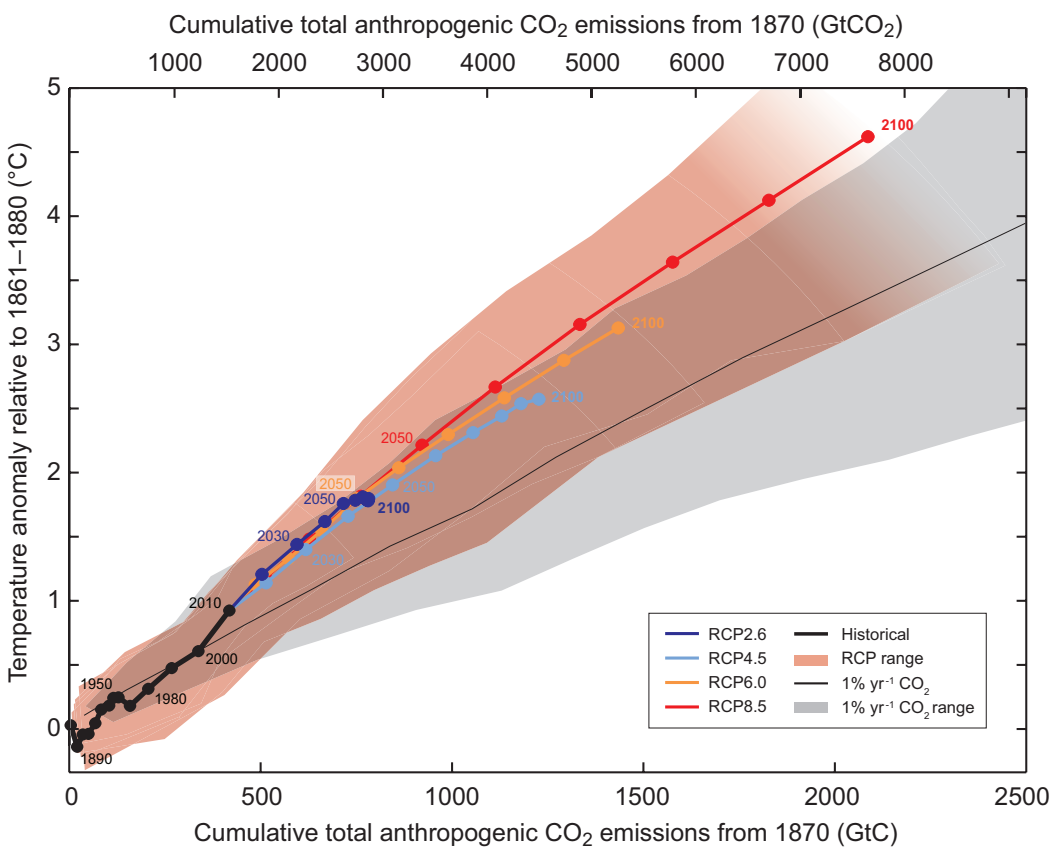

Figure SPM.10 | Global mean surface temperature increase as a function of cumulative total global CO_2 emissions from various lines of evidence. Multi-model results from a hierarchy of climate-carbon cycle models for each RCP until 2100 are shown with coloured lines and decadal means (dots). Some decadal means are labeled for clarity (e.g., 2050 indicating the decade 2040–2049). Model results over the historical period (1860 to 2010) are indicated in black. The coloured plume illustrates the multi-model spread over the four RCP scenarios and fades with the decreasing number of available models in RCP8.5. The multi-model mean and range simulated by CMIP5 models, forced by a CO_2 increase of 1% per year (1% yr^{-1} CO_2 simulations), is given by the thin black line and grey area. For a specific amount of cumulative CO_2 emissions, the 1% per year CO_2 simulations exhibit lower warming than those driven by RCPs, which include additional non-CO_2 forcings. Temperature values are given relative to the 1861–1880 base period, emissions relative to 1870. Decadal averages are connected by straight lines. For further technical details see the Technical Summary Supplementary Material. {Figure 12.45; TS TFE.8, Figure 1}

- Sustained mass loss by ice sheets would cause larger sea level rise, and some part of the mass loss might be irreversible. There is *high confidence* that sustained warming greater than some threshold would lead to the near-complete loss of the Greenland ice sheet over a millennium or more, causing a global mean sea level rise of up to 7 m. Current estimates indicate that the threshold is greater than about 1°C (*low confidence*) but less than about 4°C (*medium confidence*) global mean warming with respect to pre-industrial. Abrupt and irreversible ice loss from a potential instability of marine-based sectors of the Antarctic ice sheet in response to climate forcing is possible, but current evidence and understanding is insufficient to make a quantitative assessment. {5.8, 13.4, 13.5}

- Methods that aim to deliberately alter the climate system to counter climate change, termed geoengineering, have been proposed. Limited evidence precludes a comprehensive quantitative assessment of both Solar Radiation Management (SRM) and Carbon D ioxide Removal (CDR) and their impact on the climate system. CDR methods have biogeochemical and technological limitations to their potential on a global scale. There is insufficient knowledge to quantify how much CO_2 emissions could be partially offset by CDR on a century timescale. Modelling indicates that SRM methods, if realizable, have the potential to substantially offset a global temperature rise, but they would also modify the global water cycle, and would not reduce ocean acidification. If SRM were terminated for any reason, there is *high confidence* that global surface temperatures would rise very rapidly to values consistent with the greenhouse gas forcing. CDR and SRM methods carry side effects and long-term consequences on a global scale. {6.5, 7.7}

Box SPM.1: Representative Concentration Pathways (RCPs)

Climate change projections in IPCC Working Group I require information about future emissions or concentrations of greenhouse gases, aerosols and other climate drivers. This information is often expressed as a scenario of human activities, which are not assessed in this report. Scenarios used in Working Group I have focused on anthropogenic emissions and do not include changes in natural drivers such as solar or volcanic forcing or natural emissions, for example, of CH_4 and N_2O.

For the Fifth Assessment Report of IPCC, the scientific community has defined a set of four new scenarios, denoted Representative Concentration Pathways (RCPs, see Glossary). They are identified by their approximate total radiative forcing in year 2100 relative to 1750: 2.6 W m^{-2} for RCP2.6, 4.5 W m^{-2} for RCP4.5, 6.0 W m^{-2} for RCP6.0, and 8.5 W m^{-2} for RCP8.5. For the Coupled Model Intercomparison Project Phase 5 (CMIP5) results, these values should be understood as indicative only, as the climate forcing resulting from all drivers varies between models due to specific model characteristics and treatment of short-lived climate forcers. These four RCPs include one mitigation scenario leading to a very low forcing level (RCP2.6), two stabilization scenarios (RCP4.5 and RCP6), and one scenario with very high greenhouse gas emissions (RCP8.5). The RCPs can thus represent a range of 21st century climate policies, as compared with the no-climate policy of the Special Report on Emissions Scenarios (SRES) used in the Third Assessment Report and the Fourth Assessment Report. For RCP6.0 and RCP8.5, radiative forcing does not peak by year 2100; for RCP2.6 it peaks and declines; and for RCP4.5 it stabilizes by 2100. Each RCP provides spatially resolved data sets of land use change and sector-based emissions of air pollutants, and it specifies annual greenhouse gas concentrations and anthropogenic emissions up to 2100. RCPs are based on a combination of integrated assessment models, simple climate models, atmospheric chemistry and global carbon cycle models. While the RCPs span a wide range of total forcing values, they do not cover the full range of emissions in the literature, particularly for aerosols.

Most of the CMIP5 and Earth System Model simulations were performed with prescribed CO_2 concentrations reaching 421 ppm (RCP2.6), 538 ppm (RCP4.5), 670 ppm (RCP6.0), and 936 ppm (RCP 8.5) by the year 2100. Including also the prescribed concentrations of CH_4 and N_2O, the combined CO_2-equivalent concentrations are 475 ppm (RCP2.6), 630 ppm (RCP4.5), 800 ppm (RCP6.0), and 1313 ppm (RCP8.5). For RCP8.5, additional CMIP5 Earth System Model simulations are performed with prescribed CO_2 emissions as provided by the integrated assessment models. For all RCPs, additional calculations were made with updated atmospheric chemistry data and models (including the Atmospheric Chemistry and Climate component of CMIP5) using the RCP prescribed emissions of the chemically reactive gases (CH_4, N_2O, HFCs, NO_x, CO, NMVOC). These simulations enable investigation of uncertainties related to carbon cycle feedbacks and atmospheric chemistry.

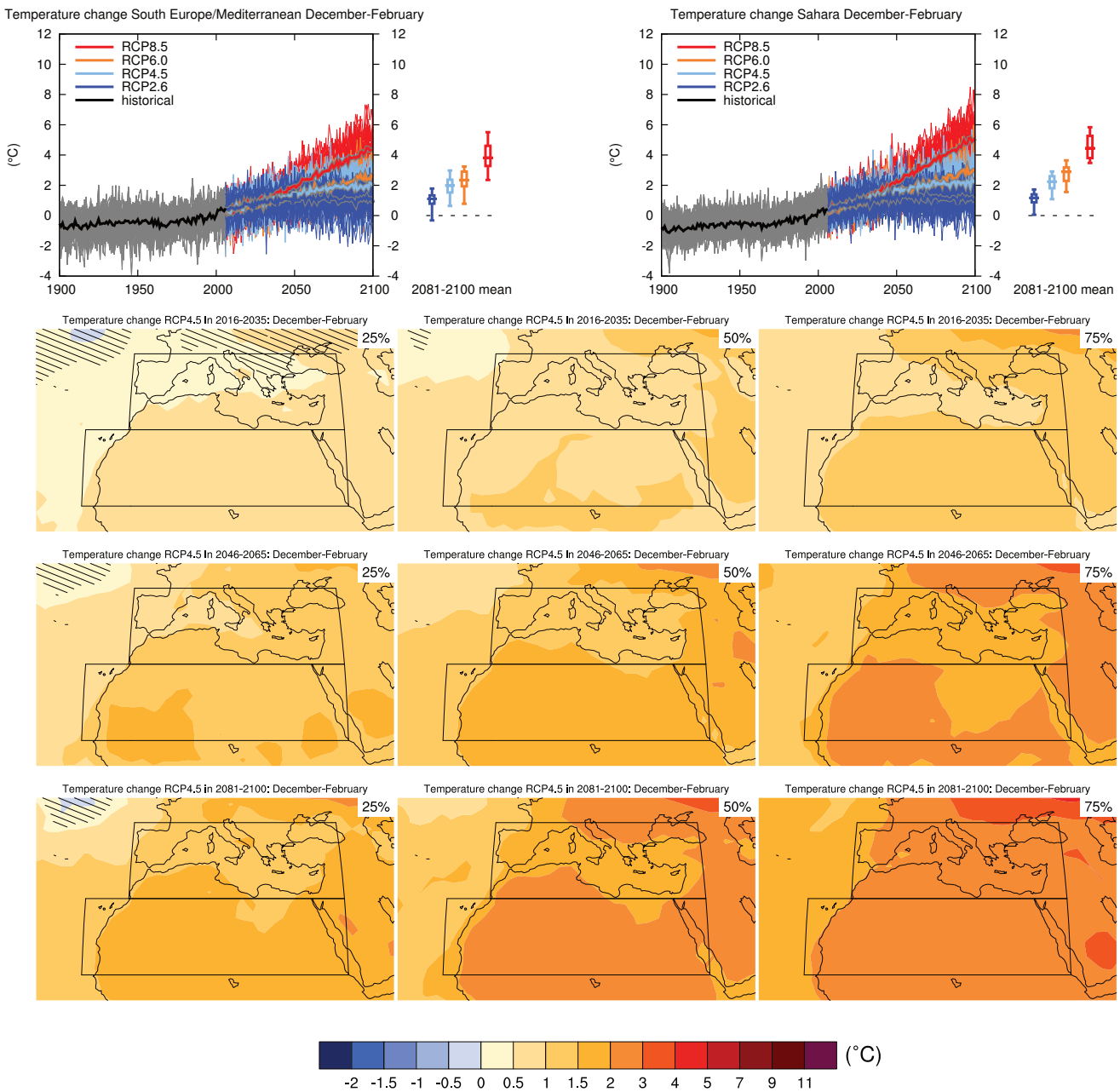

Figure AI.40 | (Top left) Time series of temperature change relative to 1986–2005 averaged over land grid points in the region South Europe/Mediterranean (30°N to 45°N, 10°W to 40°E) in December to February. (Top right) Same for land grid points in the Sahara (15°N to 30°N, 20°W to 40°E). Thin lines denote one ensemble member per model, thick lines the CMIP5 multi-model mean. On the right-hand side the 5th, 25th, 50th (median), 75th and 95th percentiles of the distribution of 20-year mean changes are given for 2081–2100 in the four RCP scenarios.

(Below) Maps of temperature changes in 2016–2035, 2046–2065 and 2081–2100 with respect to 1986–2005 in the RCP4.5 scenario. For each point, the 25th, 50th and 75th percentiles of the distribution of the CMIP5 ensemble are shown; this includes both natural variability and inter-model spread. Hatching denotes areas where the 20-year mean differences of the percentiles are less than the standard deviation of model-estimated present-day natural variability of 20-year mean differences.

Sections 9.4.1.1, 9.6.1.1, 10.3.1.1.4, Box 11.2, 14.8.6, 14.8.7 contain relevant information regarding the evaluation of models in this region, the model spread in the context of other methods of projecting changes and the role of modes of variability and other climate phenomena.

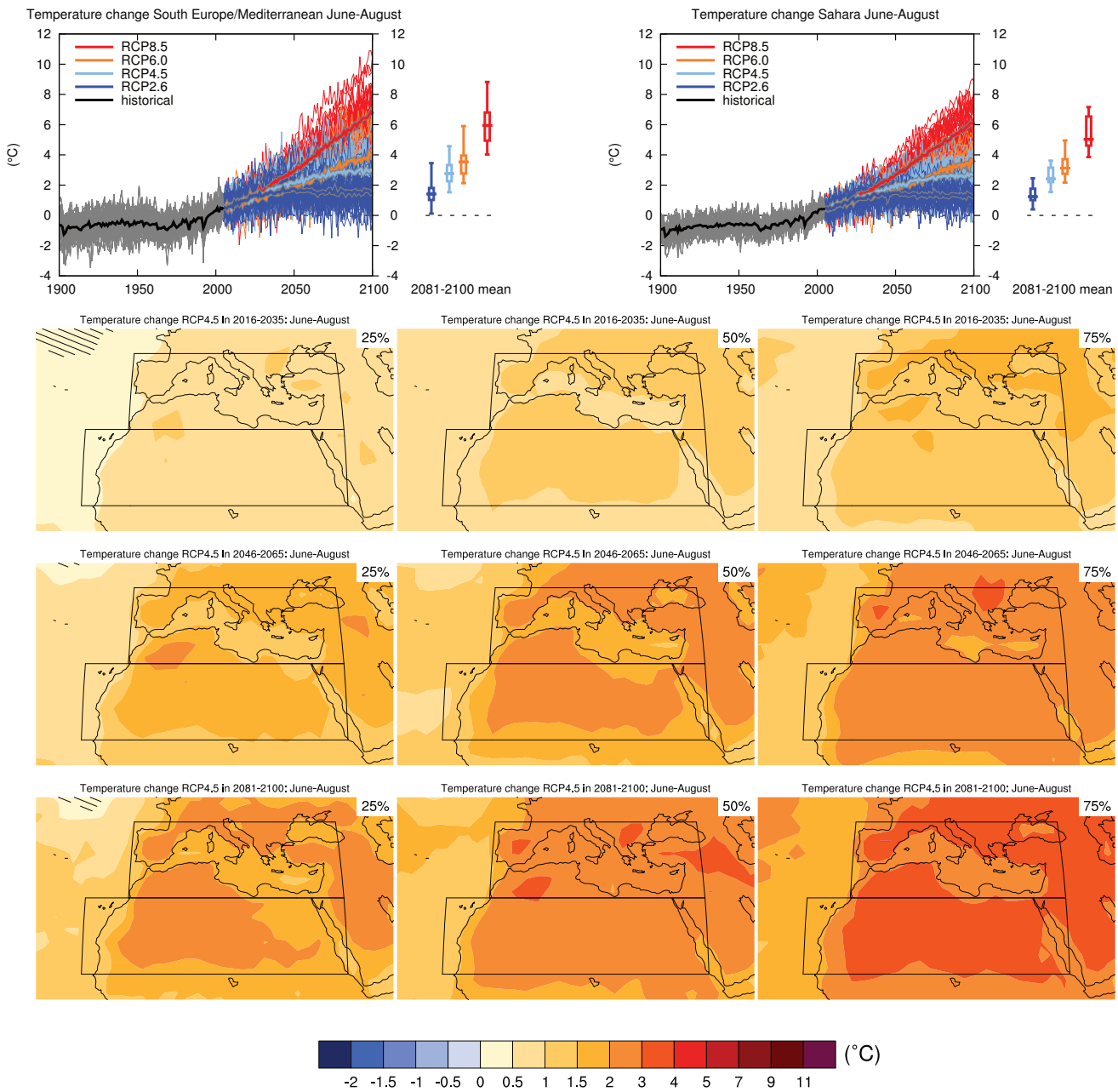

Figure AI.41 | (Top left) Time series of temperature change relative to 1986–2005 averaged over land grid points in the region South Europe/Mediterranean (30°N to 45°N, 10°W to 40°E) in June to August. (Top right) Same for land grid points in the Sahara (15°N to 30°N, 20°W to 40°E). Thin lines denote one ensemble member per model, thick lines the CMIP5 multi-model mean. On the right-hand side the 5th, 25th, 50th (median), 75th and 95th percentiles of the distribution of 20-year mean changes are given for 2081–2100 in the four RCP scenarios.

(Below) Maps of temperature changes in 2016–2035, 2046–2065 and 2081–2100 with respect to 1986–2005 in the RCP4.5 scenario. For each point, the 25th, 50th and 75th percentiles of the distribution of the CMIP5 ensemble are shown; this includes both natural variability and inter-model spread. Hatching denotes areas where the 20-year mean differences of the percentiles are less than the standard deviation of model-estimated present-day natural variability of 20-year mean differences.

Sections 9.4.1.1, 9.6.1.1, 10.3.1.1.4, Box 11.2, 14.8.6, 14.8.7 contain relevant information regarding the evaluation of models in this region, the model spread in the context of other methods of projecting changes and the role of modes of variability and other climate phenomena.

From the full, 1552 pages, 2014 report

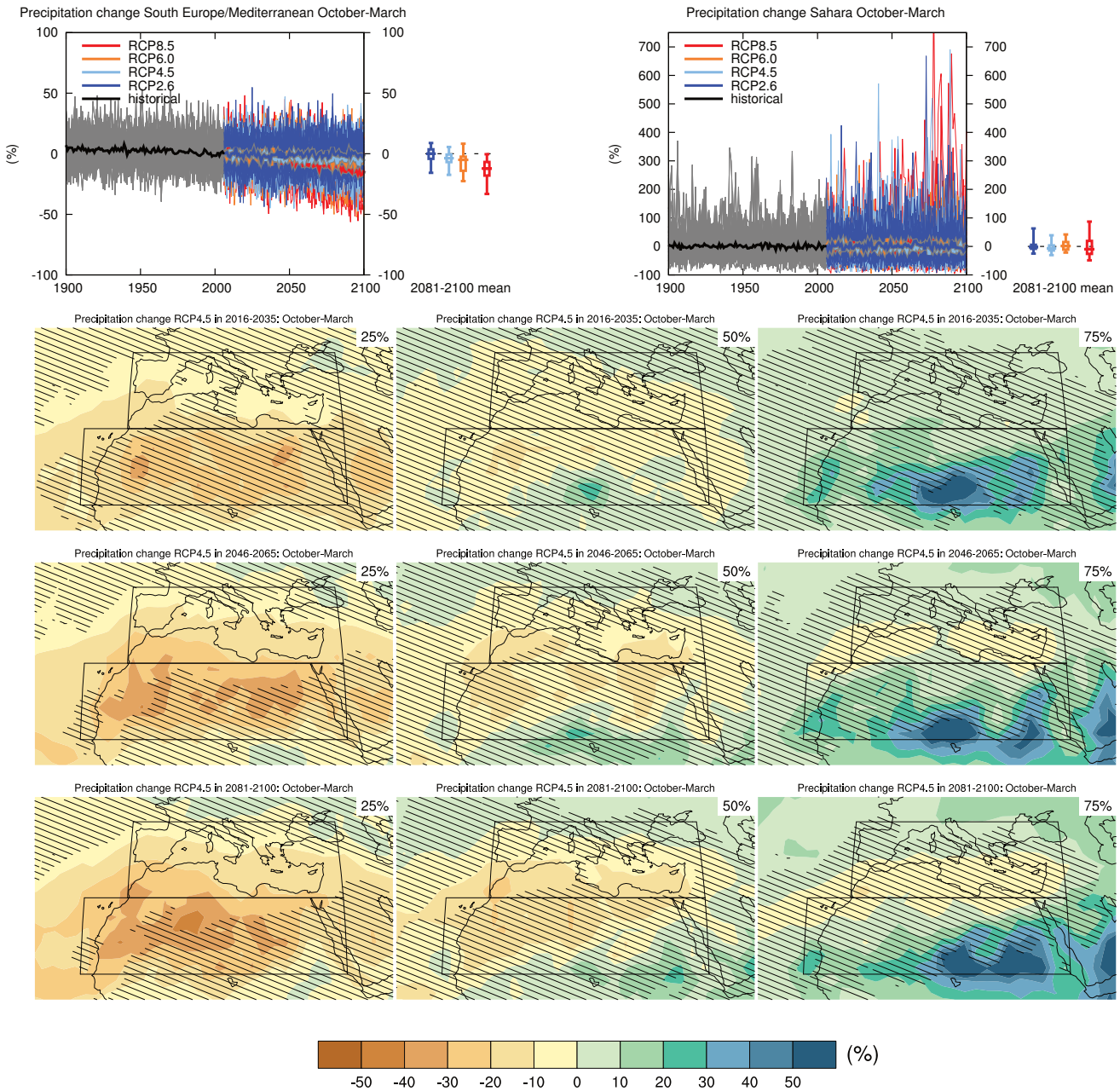

Figure AI.42 | (Top left) Time series of relative change relative to 1986–2005 in precipitation averaged over land grid points in the region South Europe/Mediterranean (30°N to 45°N, 10°W to 40°E) in October to March. (Top right) Same for land grid points in the Sahara (15°N to 30°N, 20°W to 40°E). Thin lines denote one ensemble member per model, thick lines the CMIP5 multi-model mean. On the right-hand side the 5th, 25th, 50th (median), 75th and 95th percentiles of the distribution of 20-year mean changes are given for 2081–2100 in the four RCP scenarios. Note different scales.

(Below) Maps of precipitation changes in 2016–2035, 2046–2065 and 2081–2100 with respect to 1986–2005 in the RCP4.5 scenario. For each point, the 25th, 50th and 75th percentiles of the distribution of the CMIP5 ensemble are shown; this includes both natural variability and inter-model spread. Hatching denotes areas where the 20-year mean differences of the percentiles are less than the standard deviation of model-estimated present-day natural variability of 20-year mean differences.

Sections 9.4.1.1, 9.6.1.1, Box 11.2, 12.4.5.2, 14.8.6, 14.8.7 contain relevant information regarding the evaluation of models in this region, the model spread in the context of other methods of projecting changes and the role of modes of variability and other climate phenomena.

From the full, 1552 pages, 2014 report

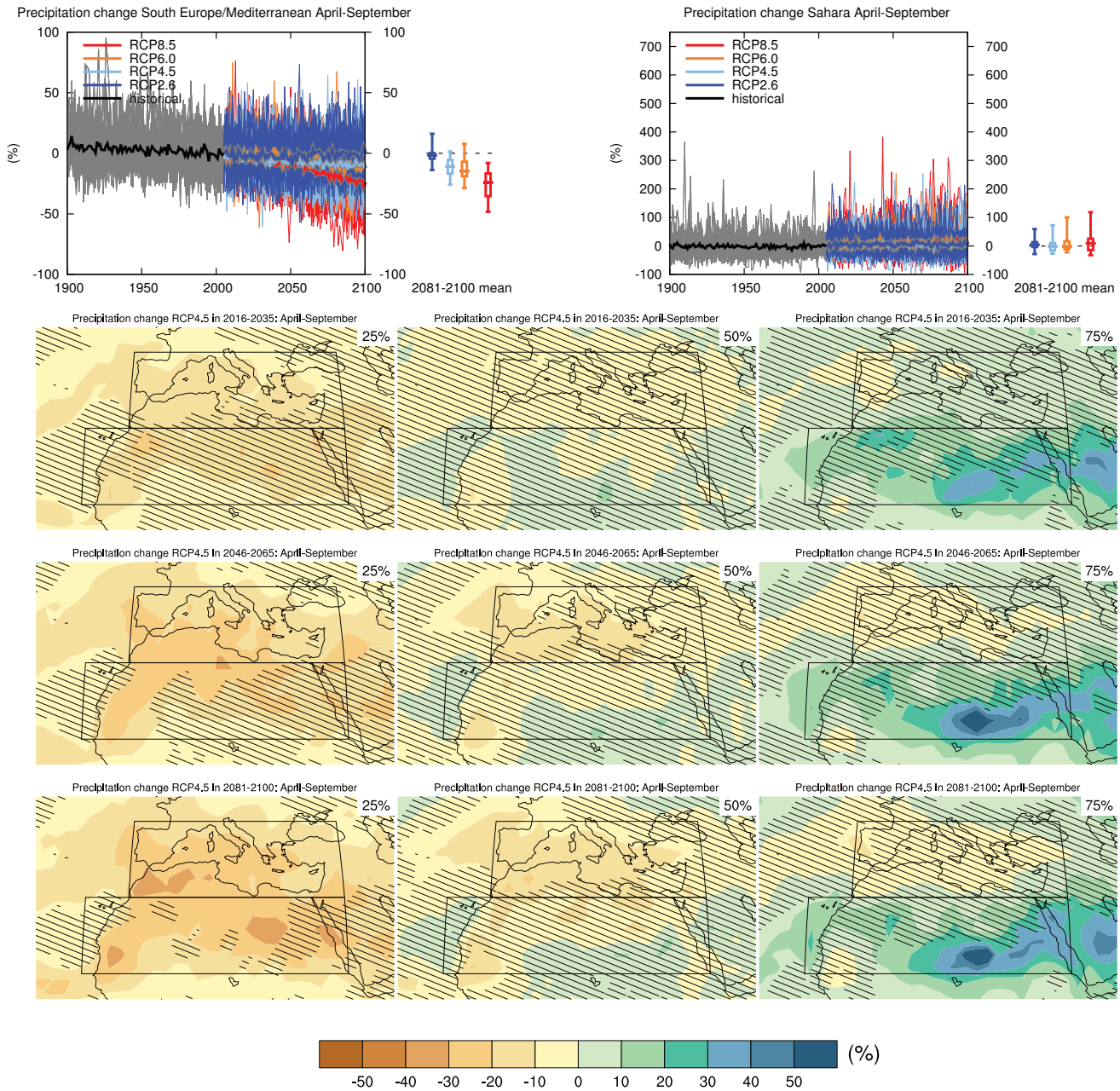

Figure AI.43 | (Top left) Time series of relative change relative to 1986–2005 in precipitation averaged over land grid points in the region South Europe/Mediterranean (30°N to 45°N, 10°W to 40°E) in April to September. (Top right) Same for land grid points in the Sahara (15°N to 30°N, 20°W to 40°E). Thin lines denote one ensemble member per model, thick lines the CMIP5 multi-model mean. On the right-hand side the 5th, 25th, 50th (median), 75th and 95th percentiles of the distribution of 20-year mean changes are given for 2081–2100 in the four RCP scenarios. Note different scales.

(Below) Maps of precipitation changes in 2016–2035, 2046–2065 and 2081–2100 with respect to 1986–2005 in the RCP4.5 scenario. For each point, the 25th, 50th and 75th percentiles of the distribution of the CMIP5 ensemble are shown; this includes both natural variability and inter-model spread. Hatching denotes areas where the 20-year mean differences of the percentiles are less than the standard deviation of model-estimated present-day natural variability of 20-year mean differences.

Sections 9.4.1.1, 9.6.1.1, Box 11.2, 12.4.5.2, 14.8.6, 14.8.7 contain relevant information regarding the evaluation of models in this region, the model spread in the context of other methods of projecting changes and the role of modes of variability and other climate phenomena.

From the full, 1552 pages, 2014 report